Supporting Information for:

Valence tautomerism in a [2×2] Co_4 grid complex containing a ditopic arylazo ligand

Nico M. Bonanno,[a] Zackery Watts,[a] Cole Mauws,[b] Brian O. Patrick,[d] Christopher R. Wiebe,[b,c] Yuki Shibano,[e] Kenji Sugisaki,[e*] Hideto Matsuoka,[e] Daisuke Shiomi,[e] Kazunobu Sato,[e*] Takeji Takui,[e*] and Martin T. Lemaire[a]*.

[a]*Department of Chemistry, Brock University, St. Catharines, ON, L2S 3A1.*
[b]*Department of Chemistry, University of Manitoba, Winnipeg, MB, R3T 2N2.*
[c]*Department of Chemistry, University of Winnipeg, Winnipeg, MB, R3B 2E9.*
[d]*Department of Chemistry, University of British of Columbia, Vancouver, BC, V6T 1Z1.*
[e]*Department of Chemistry and Molecular Materials Science, Graduate School of Science, Osaka City University, Osaka 558 8585, Japan.*

Table of Contents

Experimental Section **S2-S6**
Scheme S1. Preparation of H_2L^1. **S7**
Figure S1. ^{1}H NMR spectrum of H_2L^1 ($CDCl_3$). **S8**
Figure S2. ^{13}C NMR spectrum of H_2L^1 ($CDCl_3$). **S9**
Figure S3. FT-IR spectrum of H_2L^1 (KBr). **S10**
Figure S4. UV-visible spectrum of H_2L^1 (CH_2Cl_2). **S11**
Figure S5. ESI mass spectrum (positive ion mode) of H_2L^1. **S12**
Figure S6. Differential pulse voltammograms of H_2L^1 in CH_2Cl_2. **S13**
Figure S7. Cyclic voltammograms of H_2L^1 in CH_2Cl_2. **S13**
Figure S8. Calculated structures (BP86/def2-SVP) of $L^{3\cdot-}$ (S = 1/2). **S14**
Table S1. Atomic coordinates of the radical anion of $L^{3\cdot-}$ (S = ½). **S15**
Figure S9. Spin density distribution in $L^{3\cdot-}$ (S = ½) (B3LYP/def2-TZVPP). **S18**
Table S2. Selected calculated electronic transitions of $\mathbf{L^{3\cdot-}}$. **S19**
Table S3. Crystal data and structure refinement for **1**. **S20**
Table S4. Bond lengths (Å) and angles (°) for **1**. **S21**
Figure S10. Molecular structure of the second crystallographically independent molecule of **1**. **S24**
Figure S11. Thermogravimetric analysis of **1**. **S25**
Figure S12. UV-vis-NIR spectra of **1** (CH_2Cl_2) obtained over a 24 h period. **S26**
Figure S13. (Top) Positive ion mode ESI mass spectrum of **1** (fresh solution). (Bottom) Experimental and calculated isotopic distribution of the M^+ cluster of peaks from the ESI. **S27**
Figure S14. Positive ion mode ESI mass spectrum of **1** (in solution for 24 hours). **S28**
Figure S15. (Top) Variable temperature UV-visible-NIR spectra of **1** in THF (298 – 333 K). (Bottom) Variable temperature UV-visible-NIR spectra of **1** in Toluene (298 – 373 K). **S29**
Figure S16. Cyclic voltammogram of **1** in CH_2Cl_2 (containing 0.5 M Bu_4NPF_6). Scan rate 100 mV/s. Potential window = +1000 mV to -2000 mV. **S30**
Table S5. Electrochemical data for complex **1.** **S30**
Table S6. Crystallographic parameters for $\mathbf{[Co(L^2)_2]ClO_4}$. **S31**
Table S7. Bond distances (Å) and angles (°) for $\mathbf{[Co(L_2)^2]ClO_4}$. **S32**
Figure S17. Molecular structure of $\mathbf{[Co(L_2)^2]ClO_4}$. **S34**
Figure S18. ^{1}H NMR spectrum of $\mathbf{[Co(L_2)^2]ClO_4}$ ($CDCl_3$). **S35**
Figure S19. ^{13}C NMR spectrum of $\mathbf{[Co(L_2)^2]ClO_4}$ ($CDCl_3$). **S36**
Figure S20. ESI mass spectrum (positive ion mode) of $\mathbf{[Co(L^2)_2]ClO_4}$. **S37**
Figure S21. Spin density (red = alpha spin density and blue = beta spin density) in the S = 2 state of **1** (BP86/def2-SVP). **S38**
Table S8. Energies (E) and spin expectation values ($\langle S^2 \rangle$) for the S = 2 and broken symmetry M_S = 0 states (ααββ and αβαβ configurations) of complex **1** (BP86/def2-SVP). **S38**
Figure S22. Temperature dependence of X-band EPR spectra of complex **1**. (a) Normalized spectra between 4 K and 290 K, (b) Spectra between 100 K and 300 K. **S39**
Figure S23: Variable temperature infrared spectra of **1** (KBr pellet) **S40**
Figure S24: Variable temperature infrared spectra of **1** (KBr pellet) **S40**
References in the Supporting Information **S41**

Experimental section

General considerations

All reagents were commercially available and used as received. Anhydrous solvents (CH_2Cl_2, THF, toluene) were obtained by distillation over CaH_2. $^1H/^{13}C$-NMR spectra were recorded using either a Bruker Avance III HD 400 Digital NMR spectrometer with a 9.4 T Ascend magnet or a Bruker Avance AV 600 Digital NMR spectrometer with a 14.1 Tesla Ultrashield Plus magnet using deuterated solvents. FT-IR spectra were recorded with a Shimadzu IRAffinity spectrometer as KBr discs and UV/Vis/NIR spectra were obtained with a Shimadzu 3600 UV-Vis-NIR spectrophotometer in CH_2Cl_2 solution using quartz cuvettes. Variable temperature infrared spectra were obtained with a Specac variable temperature cell holder with temperature controller. Cyclic voltammetry (CV) and differential pulse voltammetry (DPV) experiments were performed with a Bioanalytical Systems Inc. (BASI) Epsilon electrochemical workstation. Complex **1** and **H_2L** were dissolved in anhydrous solvent (CH_2Cl_2) and sparged with N_2 gas for 10 min. Solution concentrations were approximately 10^{-3} M in **1** or **H_2L^1** containing approximately 0.5 M $^nBu_4NPF_6$. A three-electrode set-up was used including a glassy carbon working electrode, Ag/AgCl reference electrode, and a platinum wire auxiliary electrode. The scan rate for all CV experiments was 100 mV/s. For DPV experiments pulse amplitude was 50 mV, pulse width was 50 ms and step potential was 4 mV. ESI mass spectra were obtained with a Bruker HCT Plus Proteineer LC-MS with electrospray and a syringe pump was used for direct sample infusion. A QD-MPMS SQUID magnetometer was used to record the variable temperature magnetic susceptibility properties of **1** at an external magnetic field of 10 kOe over a temperature range of 2-400K. The sample was weighed into a polycarbonate cap and diamagnetic contributions were calculated using Pascal's constants. Microanalyses were performed by Atlantic Microlab, Inc. (Norcross, GA, USA). X-band EPR spectra were recorded using a Bruker Elexsys E600 spectrometer. Thermal gravimetric

analysis was performed using a Perkin-Elmer STA 8000 instrument over a temperature range of 30 to 1600ºC.

Theoretical calculations. All theoretical calculations were performed with the programs ORCA 4.1.1[1]. Geometry optimization and frequency calculations on $\mathbf{L}^{3-\cdot}$ trianion radical were run using the BP86[2–4] functional and def2-SVP[5,6] basis set on all atoms. Broken-symmetry DFT[7-9] (complex **1**) and TD-DFT ($\mathbf{L}^{3-\cdot}$) calculations were run using the BP86[2,4] functional with the def2-SVP[5,6] (complex **1**) or def2-TZVPP[6] ($\mathbf{L}^{3-\cdot}$) basis set on all atoms. In the TD-DFT calculations the polarized continuum model (PCM) was used to model the solvent environment (THF) and 50 transitions were calculated. Tight SCF convergence criteria were used for all calculations. The program QMForge[10] was used to analyse the TD-DFT results.

Synthesis

4,6-dihydrazine-1,3-pyrimidine. Methanol (75 mL) was added to hydrazine monohydrate (90 mL), and the mixture was cooled to 10 °C. 4,6-dichloropyrimidine (25.0 g, 168 mmol) was slowly added (internal temperature 20 °C or lower) and the resulting mixture was heated to reflux and left to react for approximately 12 h. The reaction mixture was cooled to slightly above room temperature and filtered using a Buchner funnel. The white solid was rinsed with isopropanol (4 x 50 mL), and then dried. Yield, 18.6 g (79%). Spectroscopic data matched reported values. ^{1}H-NMR (400 MHz, d_6-DMSO) 7.82 (s, 1H), 7.55 (s, 2H), 5.96 (s, 1H), 4.12 (s, 4H).

2-{6-[2-Hydroxy-3,5-bis(*tert*-butyl)phenylazo]-4-pyrimidinylazo}-4,6-bis(*tert*-butyl)phenol ($\mathbf{H_2L^1}$). 3,5-di-*tert*-butyl-*o*-benzoquinone (5.00 g, 22.7 mmol) and 4,6-dihydrazine-1,3-pyrimidine (1.59 g, 11.3 mmol) were added to a RBF (500 mL) containing glacial acetic acid (200 mL). The solution was refluxed for approximately 24 h. This resulted in a dark red color. The flask was cooled and its contents were added to a beaker (1 L) containing approximately 300 mL

of ice water. The solution was stirred rapidly until the ice had completely melted, and then the material was slowly precipitated out of the solution by adding small quantities of $NaHCO_3$. The precipitated solid was filtered and rinsed with water (100 mL × 4) and dried. Crude yield, 4.92 g (~80%). The crude product was recrystallized by dissolving 0.200 g into 4 mL of DCM/nitromethane (1:1 mixture) in a 2 dram vial. The vial was allowed to stand with the cap off for 6 d. The crystals were isolated by vacuum filtration and washed sparingly with nitromethane. Yield, 0.043 g (22%). ^{1}H-NMR (400.25 MHz, $CDCl_3$): δ 15.25 (s, 1H), 8.97 (d, 1H, J = 0.8 Hz), 7.94 (d, 1H, J = 0.8 Hz), 7.43 (d, 2H, J = 2.5 Hz), 7.30 (d, 2H, J = 2.5 Hz), 1.44 (s, 18 H), 1.35 (s, 18 H). ^{13}C-NMR (100.65 MHz, $CDCl_3$): δ 170.3, 164.7, 159.4, 143.6, 143.2, 137.9, 134.0, 125.8, 95.2, 35.4, 34.6, 30.3, 29.4. Anal. Calc'd for % (found) $C_{32}H_{44}N_6O_2 \cdot 0.25CH_2Cl_2$: C, 68.44 (68.50); H, 7.92 (8.27); N, 14.85% (14.67). MS (ESI+): *m/z* 545.3 $[M+H^+]^+$, 567.4 $[M+Na^+]^+$, 1111.6 $[M_2 + Na^+]^+$. FT-IR (KBr, cm^{-1}): 3429 (br, w), 2997 (w), 2959 (m), 2906 (w), 2868 (w), 1577 (s), 1552 (m), 1477 (br, s), 1406 (w), 1388 (w), 1364 (w), 1339 (w), 1306 (w), 1265 (m), 1200 (m), 1121 (m), 1094 (m), 1024 (w), 974 (m), 901 (m), 874 (w), 816 (w), 637 (w), 540 (w). UV-Vis (CH_2Cl_2, λ_{max}): 363, 490 nm.

$[Co_4L^1{}_4] \cdot 1.65CH_2Cl_2 \cdot 2CH_3CN$ (1). H_2L^1 (740 mg, 1.35 mmol) was added to MeOH (80 mL) in an Erlenmeyer flask, followed by the addition of solid $Co(ClO_4)_2 \cdot 6H_2O$ (490 mg, 1.35 mmol) resulting in a very dark green color. The solution was warmed to 50° C and allowed to stir for 4 d. After this time, the brown precipitate formed in the solution was filtered and washed with MeOH (25 mL × 3). Yields of this powder ranged from approximately 20-70%. Single crystals were grown by diffusion: dissolving approximately 20 mg of the complex powder in 6 mL of DCM in a 2 dram vial, with slow diffusion of acetonitrile (approximately 15 mL placed in the outer vessel). After 10 d the single crystals are filtered and washed with acetonitrile and dried under vacuum with

mild heating (45°C) overnight. Individual experiments typically produced about 16 mg of single crystals (80%). Anal. Calc'd for % (found) $C_{128}H_{168}N_{24}O_8Co_4 \cdot 2CH_3CN \cdot 1.65CH_2Cl_2$: C, 61.06 (61.01); H, 6.80 (7.06); N, 13.85% (13.88). ESI-MS (+): *m/z* 2406.2 (M^+, 100%), 1203.1 (M^{2+}). FT-IR (KBr, cm^{-1}): 3099 (w), 2955 (s), 1607 (m), 1539 (w), 1481 (m), 1383 (m), 1256 (m), 1229 (m), 1200 (m), 1155 (m), 1124 (m), 1092 (m), 1041 (m), 1024 (m), 1011 (m), 991 (m), 933 (m), 903 (m), 733 (w), 638 (w), 542 (w), 502 (w). UV-Vis (CH_2Cl_2, λ_{max}): 560, 744, 1499 nm.

HL^2. 2-hydrazinopyridine (0.99 g, 9.08 mmol) and 3,5-di-*tert*-butyl-*o*-benzoquinone (2.00 g, 9.08 mmol) were added to a Schlenk flask (250 mL) charged with glacial acetic acid (100 mL). The solution was sparged rapidly with N_2 for 5 min and then equipped with a condenser and refluxed for 4 d under an N_2 atmosphere. The flask was cooled and its contents were added to a beaker (500 mL) containing approximately 150 mL of ice water. The solution was stirred rapidly until the ice had completely melted, and then the material was slowly precipitated by adding small quantities of $NaHCO_3$. The precipitated solid was filtered and rinsed with water (75 mL × 4) and dried. While drying it is common for the product to form a dark red oily semi-solid, although powders have also been isolated. Yields ranged from 75-90%. Spectroscopic characterization was identical to reported data.

$[Co(L^2)_2]ClO_4 \cdot EtOH \cdot 2.2H_2O$. HL^2 (200 mg, 0.638 mmol) was weighed into a tared 2 dram vial and dissolved with hexanes (3 mL). In another vial $Co(ClO_4)_2 \cdot 6H_2O$ (117 mg, 0.319 mmol) was fully dissolved in ethanol (3 mL). The metal ion solution was rapidly added by pipette to the ligand solution, which was then capped and shaken vigorously by hand for approximately 10 s resulting in a dark green solution. The vial was allowed to stand for several days resulting in large needle crystals of the desired product, which were suitable for X-ray diffraction. The crystals were filtered, and the remaining solution was left to stand for an additional 5 d. The solution was again filtered,

and the crystals were washed sparingly with hexanes. The crystals were dried overnight using a vacuum pump. Yield, 146 mg (68%). ^{1}H-NMR (600.2 MHz, CD_2Cl_2): δ 8.109-8.05 (m, 4H), 7.94 (s, 2H), 7.52-7.43 (m, 4H), 7.29 (s, 2H), 1.44 (s, 18H), 1.089 (s, 18H). ^{13}C-NMR (150.9 MHz, $CDCl_3$):δ 182.2, 169.5, 148.8, 144.8, 144.2, 143.9, 143.5, 136.6, 126.9, 122.9, 111.6, 35.15, 34. 8, 30.6, 28.7. Anal. Calc'd for % (found) $C_{38}H_{48}N_6O_6ClCo \cdot EtOH \cdot 2.5H_2O$: C, 55.55 (55.13); H, 6.81 (6.38); N, 9.72% (10.16). MS (ESI+): *m/z* 679.3 [$(M\text{-}ClO_4)^+$, 100%]. FT-IR (KBr, cm^{-1}): 3099 (w), 2959 (m), 2907 (w), 2868 (w), 1603 (w), 1549 (w), 1481 (s), 1447 (m), 1377 (s), 1364 (s), 1292 (w), 1247 (m), 1223 (s), 1196 (s), 1172 (s), 1153 (s), 1098 (s br), 1040 (w), 912 (m), 830 (w), 775 (w), 717 (w), 623 (m), 542 (w). UV-Vis (CH_2Cl_2, λ_{max}): 402, 640, 698 nm.

Scheme S1. Preparation of H_2L[1]. Reagents and conditions: (i) hydrazine hydrate, MeOH, reflux (ii) 3,5-di-*tert*-butyl-1,2-quinone, glacial acetic acid, reflux.

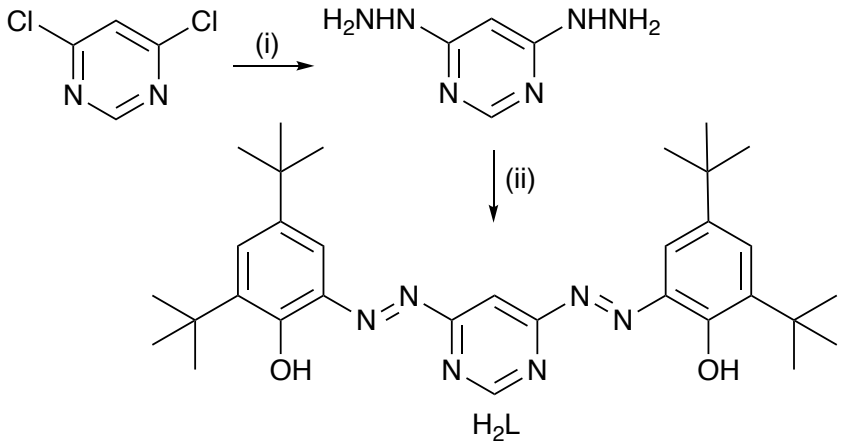

Figure S1. ^{1}H NMR spectrum of H_2L^1 ($CDCl_3$).

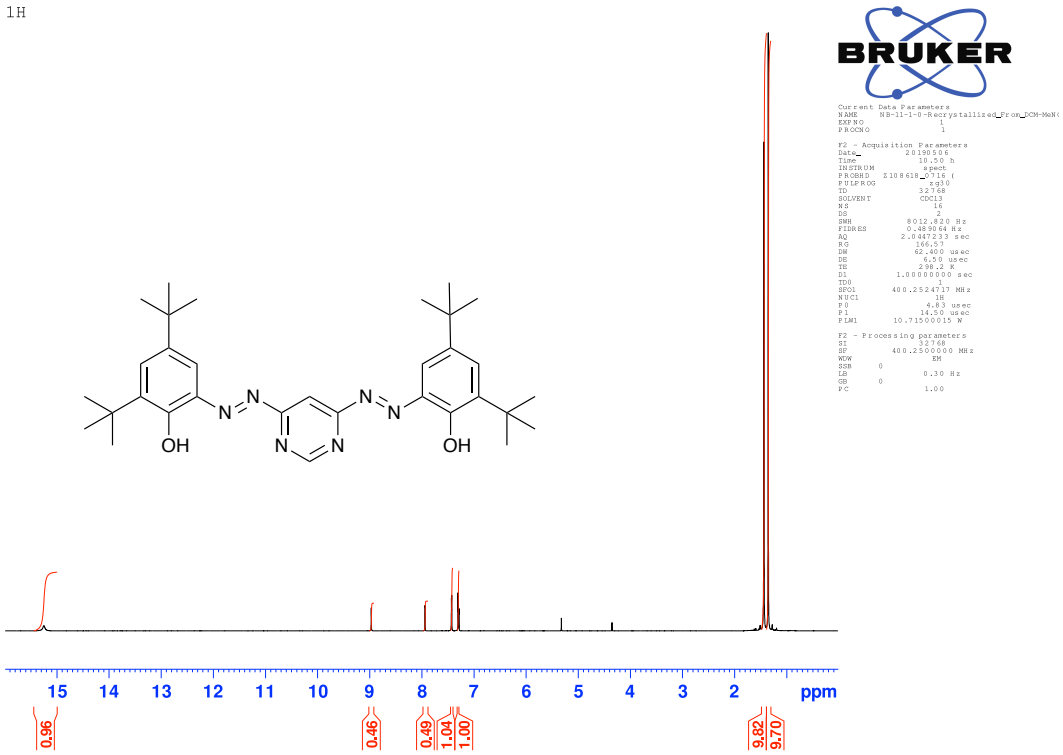

Figure S2. ^{13}C NMR spectrum of H_2L^1 ($CDCl_3$).

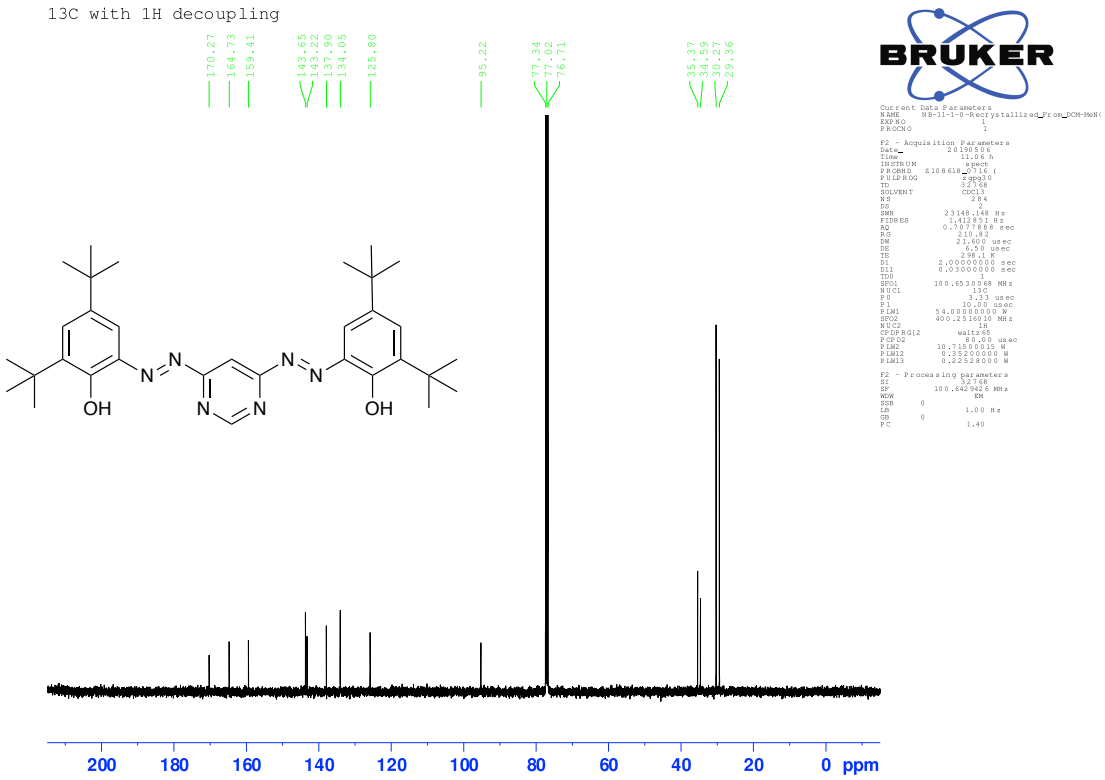

Figure S3. FT-IR spectrum of H_2L^1 (KBr).

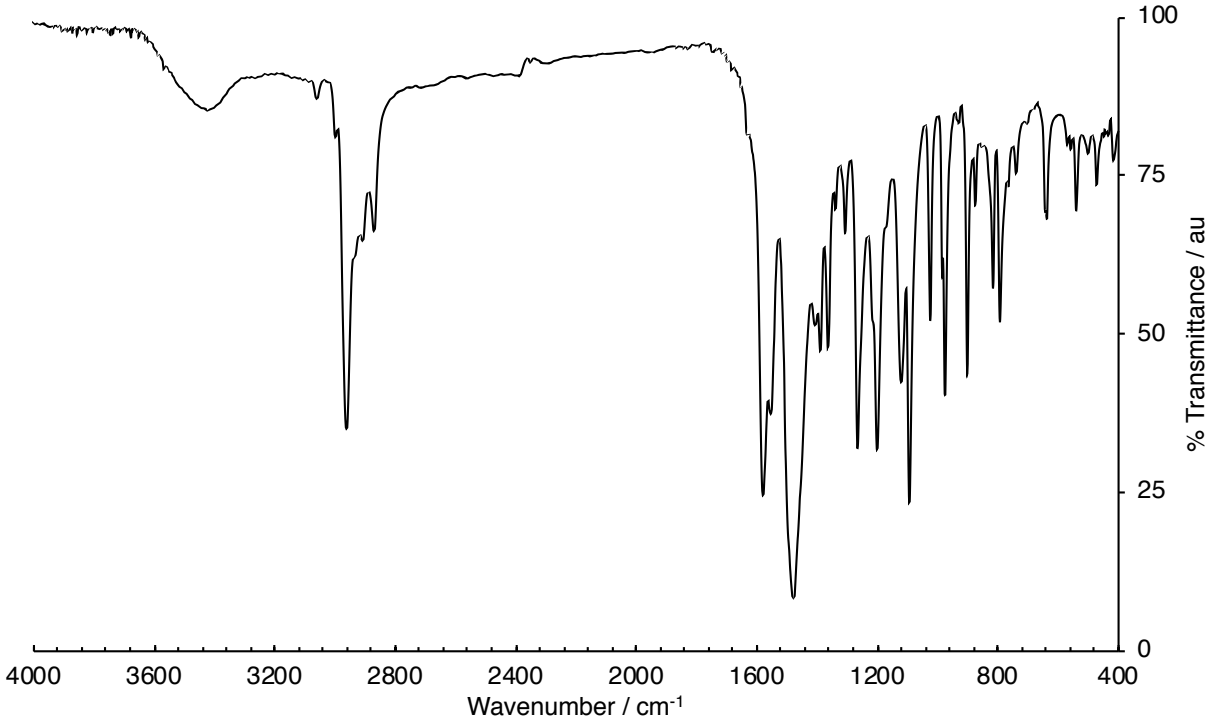

Figure S4. UV-visible spectrum of H_2L^1 (CH_2Cl_2).

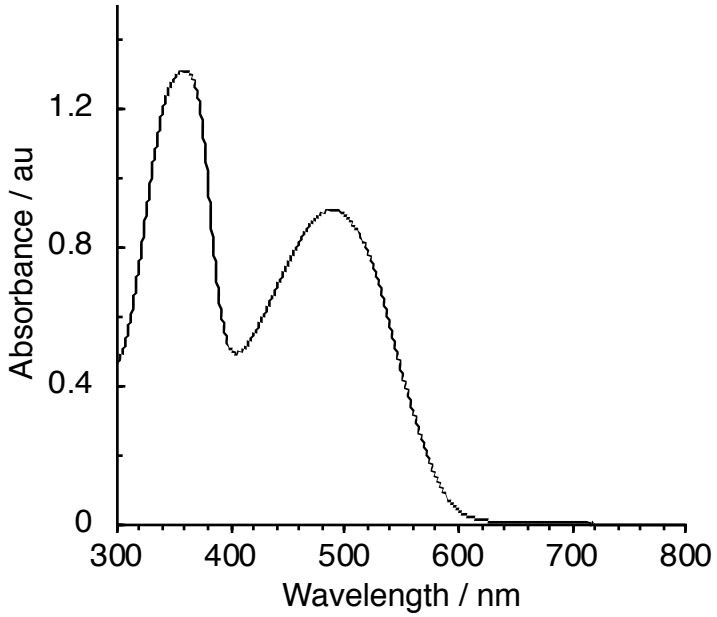

Figure S5. ESI mass spectrum (positive ion mode) of H_2L^1.

MS Instrument: Bruker HCTplus Ion-Trap

Sample Name: NB-11-1-0-DCM-MeNO2-Crystals **Ion Source Type(Polarity)**: ESI+/-

File Name: MLH2477 **Solvent** : DCM/MeOH

Please read through the 7-page report.

ESI+

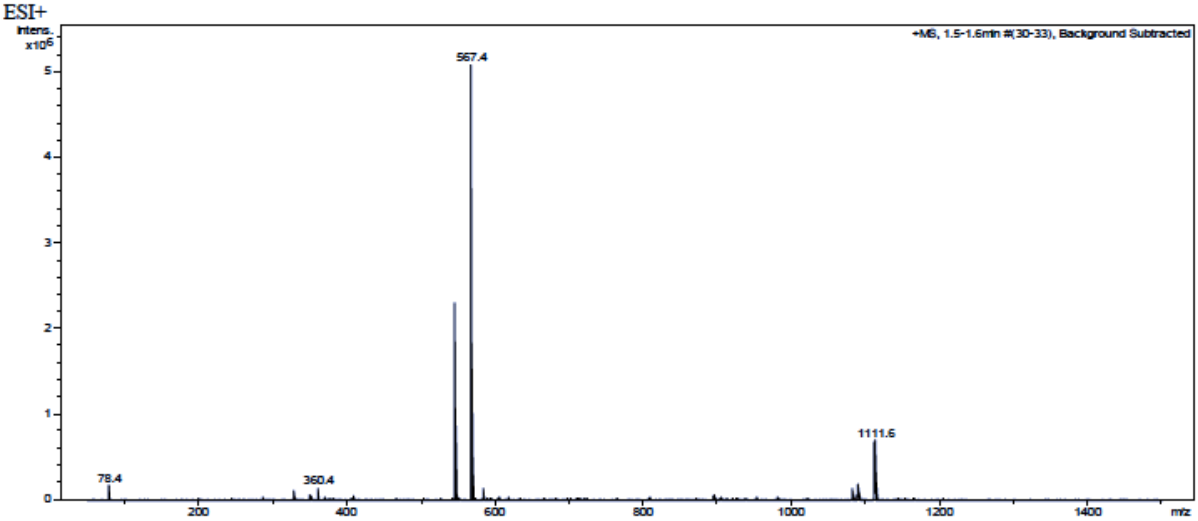

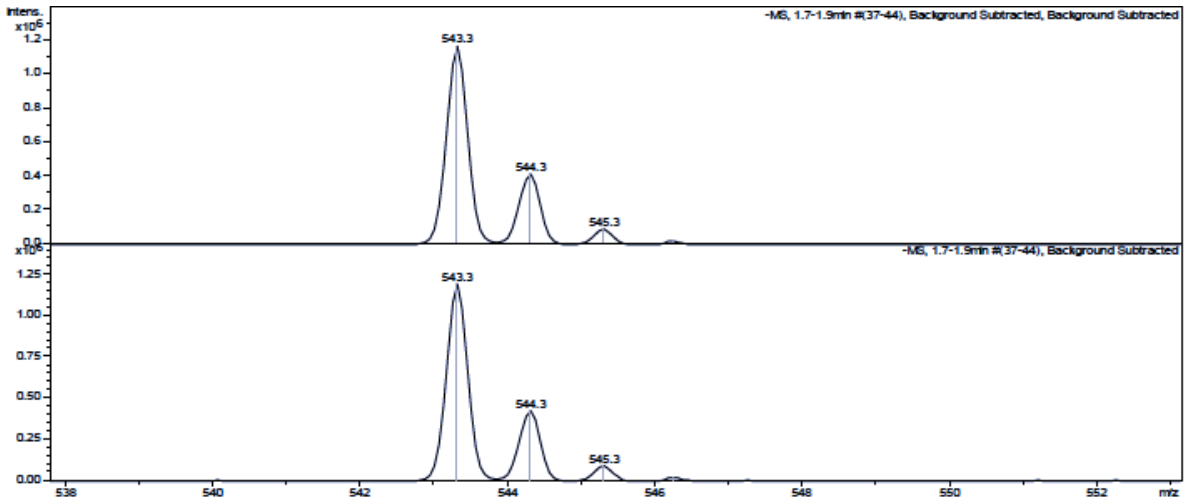

Figure S6. Differential pulse voltammograms of H_2L^1 in CH_2Cl_2.

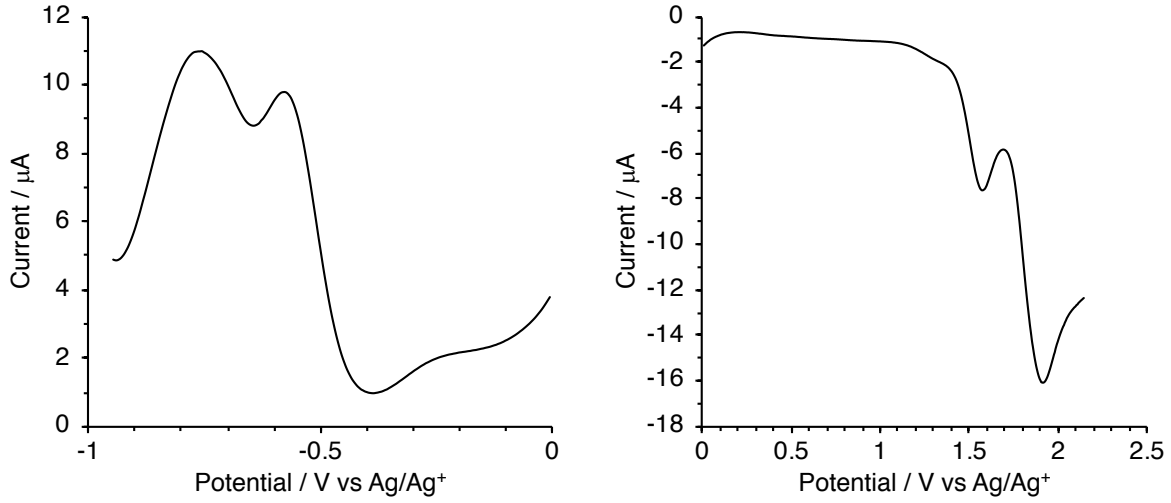

Figure S7. Cyclic voltammograms of H_2L^1 in CH_2Cl_2.

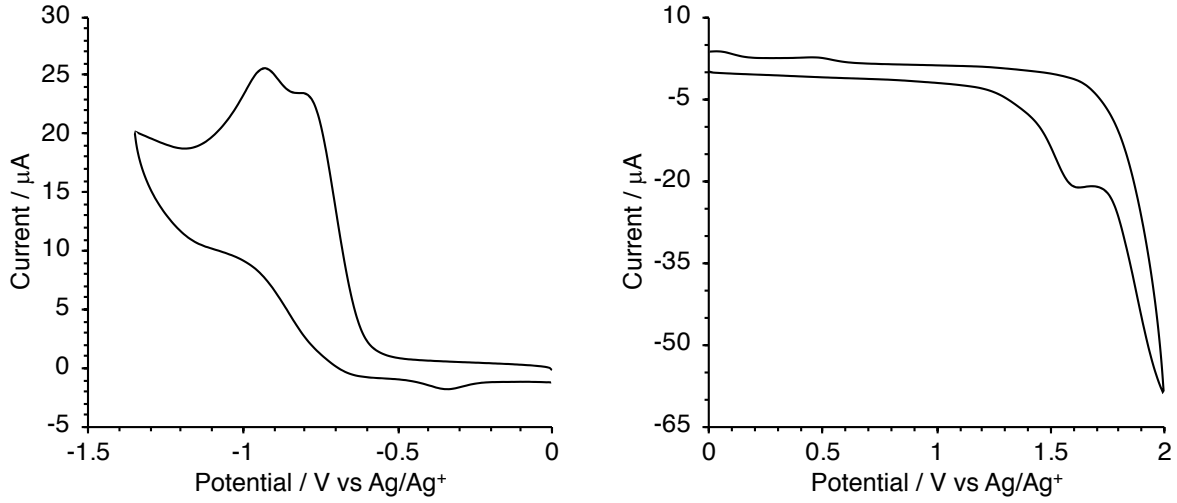

Figure S8. (Top) Calculated structures (BP86/def2-SVP) of $L^{3-\cdot}$(S = 1/2) with selected calculated bond distances (Å). (Bottom) Valence bond sketch of $L^{3-\cdot}$ in the trianion-radical oxidation state from the crystal structure of **1** (from one of two independent molecules of the complex) with bond distances.

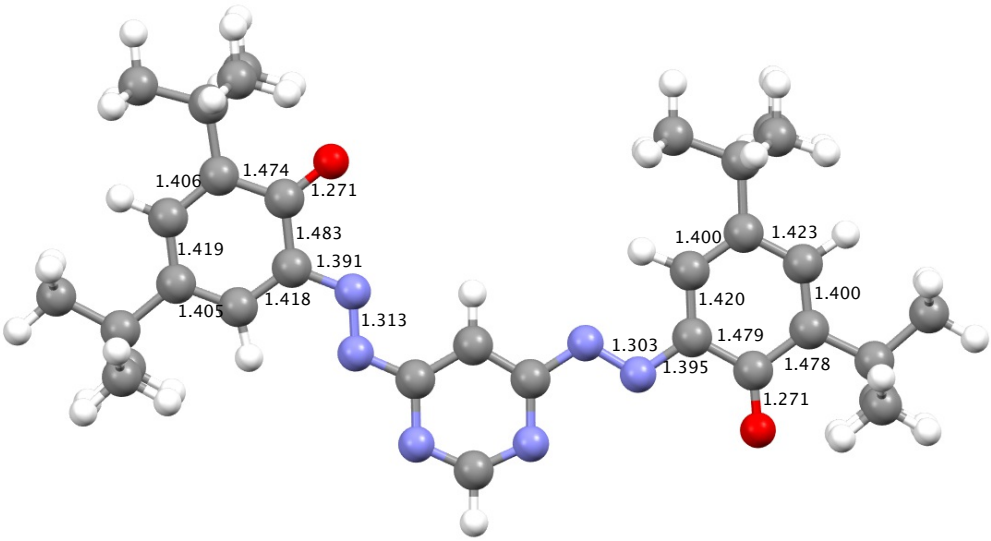

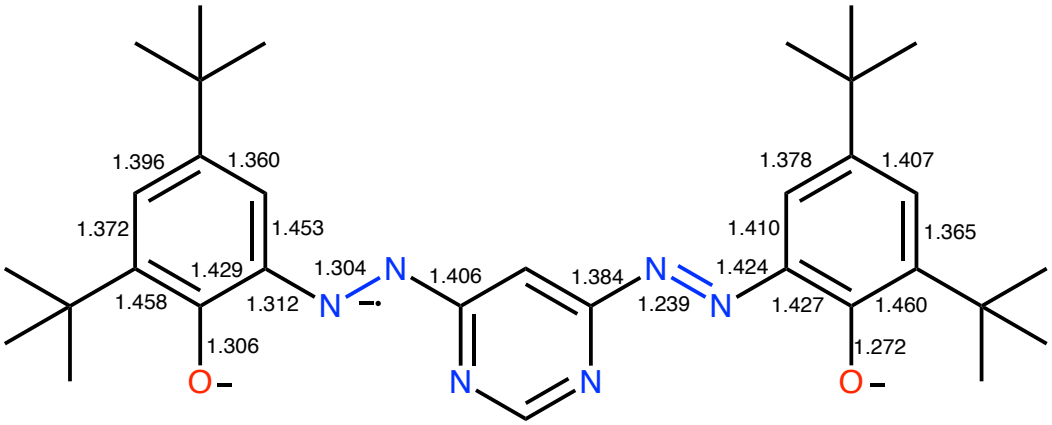

Table S1. Atomic coordinates of the radical anion of $L^{3-\cdot}$ (S = ½).

H	-0.612520	0.278300	-0.168670
C	-1.604940	0.702580	0.038710
C	-4.008300	1.725840	0.519490
C	-1.992060	1.043270	1.355750
C	-2.520030	0.909270	-1.032250
N	-3.768970	1.443840	-0.764950
N	-3.238670	1.575910	1.605640
H	-5.018500	2.158860	0.720580
N	-1.054160	0.811330	2.362280
N	-2.292430	0.616380	-2.364170
N	-1.426770	1.117990	3.573120
N	-1.108070	0.133820	-2.661660
C	-0.465250	0.879950	4.554990
C	1.454380	0.415310	6.576120
C	0.819700	0.358020	4.251670
C	-0.840350	1.198220	5.950170
C	0.209680	0.932360	6.956020
C	1.794280	0.115780	5.227220
H	0.979830	0.161090	3.180390
H	2.213690	0.227680	7.354920
O	-1.977100	1.665210	6.275930
C	-0.113170	1.241890	8.431420
C	-1.339040	0.401050	8.869390
H	-2.164770	0.618930	8.161590
H	-1.651850	0.651810	9.911280
H	-1.098600	-0.683160	8.827670
C	-0.463610	2.745160	8.568480
H	-1.287880	2.961640	7.858310
H	0.416340	3.372360	8.308820
H	-0.778770	2.995160	9.609830
C	1.054140	0.928030	9.385220
H	1.960290	1.521390	9.137330
H	1.336450	-0.146070	9.352570
H	0.762910	1.172000	10.432090
C	3.189130	-0.451740	4.903190
C	3.396380	-1.794070	5.648530
H	3.288910	-1.664150	6.745380
H	4.406040	-2.225030	5.448770
H	2.632780	-2.531350	5.325700
C	3.367770	-0.706660	3.395640
H	3.242360	0.225690	2.810230
H	2.618960	-1.429500	3.015910
H	4.381970	-1.114490	3.187290
C	4.283190	0.546800	5.357300

H	4.206420	0.759020	6.443820
H	4.165320	1.511460	4.821950
H	5.307890	0.155570	5.152850
C	-0.940030	-0.168910	-4.008470
C	-0.569760	-0.809700	-6.747080
C	0.383580	-0.688550	-4.429050
C	-1.976220	0.000030	-4.962010
C	-1.827590	-0.307450	-6.325050
C	0.506760	-1.002830	-5.863420
H	-2.915590	0.395910	-4.537670
H	-0.430050	-1.060110	-7.809340
O	1.345540	-0.851230	-3.613910
C	1.859110	-1.548880	-6.363150
C	1.873400	-1.843340	-7.874730
H	1.114050	-2.604950	-8.154430
H	2.873000	-2.232900	-8.173720
H	1.670300	-0.930740	-8.475290
C	2.187240	-2.863240	-5.610190
H	1.431630	-3.643060	-5.847250
H	2.155430	-2.644360	-4.523240
H	3.194820	-3.252980	-5.891770
C	2.969200	-0.510620	-6.060470
H	2.935180	-0.291080	-4.973730
H	2.785880	0.427360	-6.627850
H	3.977840	-0.899180	-6.340240
C	-3.013080	-0.100750	-7.288090
C	-2.667620	-0.473750	-8.742720
H	-2.369720	-1.539750	-8.827180
H	-1.825750	0.138910	-9.127340
H	-3.546560	-0.308030	-9.405960
C	-4.207000	-0.978580	-6.837920
H	-3.925450	-2.052150	-6.865340
H	-5.100410	-0.830750	-7.490730
H	-4.492430	-0.740060	-5.794390
C	-3.450300	1.384540	-7.265180
H	-3.707810	1.697800	-6.234310
H	-4.335340	1.565570	-7.920890
H	-2.619230	2.035090	-7.609760
C	1.06824	-0.21249	0.42161
C	2.90439	1.34051	2.01283
C	2.46838	-0.09909	0.05363
C	0.70544	0.34546	1.67007
C	1.60107	1.13836	2.43123
C	3.38170	0.70447	0.83191
H	1.24234	1.58384	3.37527
H	3.58889	1.96548	2.60677

C	0.15595	-0.93295	-0.51516
H	0.09787	-2.37786	-2.12910
C	0.78868	-1.76352	-1.53356
H	2.54765	-2.30919	-2.63049
C	2.12134	-1.70671	-1.81311
C	2.99924	-0.82227	-1.07696
C	4.74657	0.82953	0.43097
H	5.41649	1.46259	1.03374
C	5.22345	0.15036	-0.68348
H	6.27851	0.24631	-0.98289
C	4.35550	-0.68430	-1.42075
H	4.73959	-1.25034	-2.28412
O	-0.54553	0.09006	2.19711
N	-1.16029	-0.88180	-0.69061
N	-1.97515	-0.07315	-0.03265
C	-3.34062	-0.01280	-0.33330
C	-6.02800	0.16285	-0.91843
N	-3.80586	-0.69411	-1.39307
C	-4.16865	0.79357	0.49468
C	-5.52872	0.87586	0.18853
C	-5.11530	-0.60151	-1.66582
H	-3.74461	1.33829	1.35333
H	-6.19748	1.49173	0.81003
H	-5.46508	-1.17550	-2.54405
H	-7.09194	0.19936	-1.19492
H	-0.59538	0.49812	3.08277
H	-1.66868	0.37983	0.84597

Figure S9. Spin density distribution in $L^{3-\cdot}$ (S = ½) (B3LYP/def2-TZVPP).

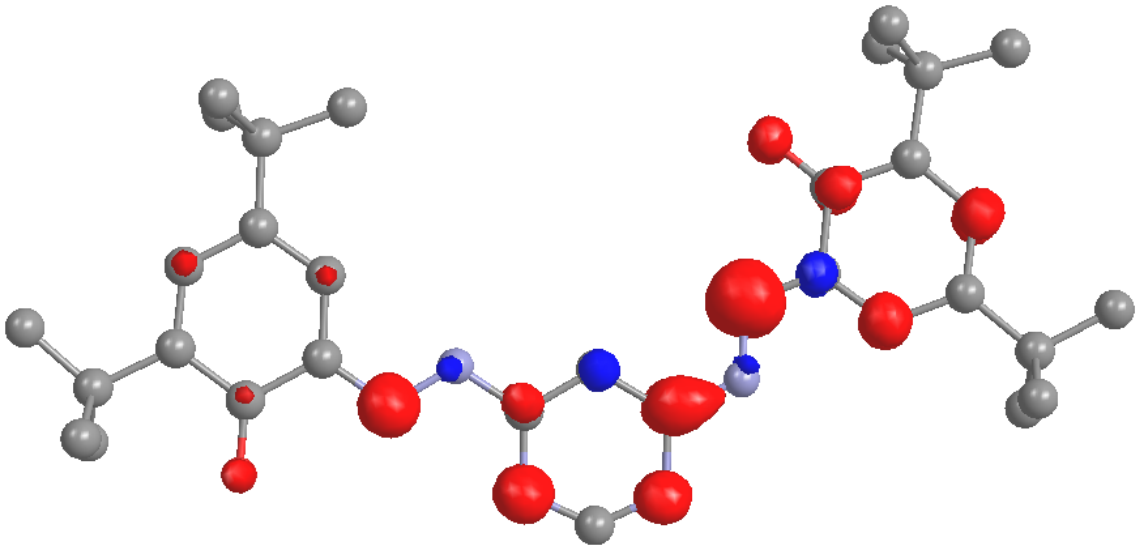

Table S2. Selected calculated electronic transitions of $\mathbf{L}^{3-\cdot}$ (B3LYP/def2-TZVPP/PCM(THF).

Energy (cm^{-1})	**λ (nm)**	**Oscillator strength**	**Main contributions (%)**
6473	1545	0.3237	αH →αL (91.6)
11515	868	0.0583	βH→βL (59.9)
13315	751	0.1541	βH→βL (30.2) βH→βL+1 (22.7) αH-1→αL (20.2)
18047	554	0.1509	βH→βL+1 (47.3) αH-2→αL (24.4)
19095	523.7	0.3014	αH→αL+1 (86.3)
19724	507	0.1144	αH-3→αL (34.3) βH-1→βL (15.1)
22963	435.5	0.2497	βH-5→βL (24.5) βH-5→βL+1 (18.1)
25485	392.4	0.1858	αH→αL+5 (30.2) βH-5→βL (23.2)
27198	367.7	0.1483	βH-5→βL+1 (32.8) αH-8→αL (23.9)
28526	350.6	0.2269	αH→αL+7 (52.9)

Table S3. Crystal data and structure refinement for **1** (CCDC 1922365).

Formula	$C_{128}H_{168}Co_4N_{24}O_8$
$D_{calc.}$/ g cm^{-3}	0.987
μ/mm^{-1}	0.453
Formula Weight	2406.57
Colour	black
Shape	blade
Size/mm^3	0.35×0.10×0.02
T/K	100(2)
Crystal System	tetragonal
Space Group	I-4
a/Å	39.4401(13)
b/Å	39.4401(13)
c/Å	10.4150(5)
α/°	90
β/°	90
γ/°	90
V/Å^3	16200.8(13)
Z	4
Z'	0.5
Wavelength/Å	0.71073
Radiation type	MoK$_\alpha$
Θ_{min}/°	2.271
Θ_{max}/°	22.779
Measured Refl.	40015
Independent Refl.	10379
Reflections with I > 2(I)	7982
R_{int}	0.1084
Parameters	834
Restraints	1551
Largest Peak	0.363
Deepest Hole	-0.403
GooF	1.030
wR_2 (all data)	0.1693
wR_2	0.1588
R_1 (all data)	0.0926
R_1	0.0681

Table S4. Bond lengths (Å) and angles (°) for **1**.

Atom	Atom	Length/Å
Co1	O1[1]	1.901(6)
Co1	O2	1.898(6)
Co1	N1[1]	1.856(8)
Co1	N3[1]	1.944(9)
Co1	N4	1.965(9)
Co1	N6	1.859(8)
O1	C1	1.306(11)
O2	C24	1.271(12)
N1	N2	1.305(11)
N1	C6	1.311(13)
N2	C16	1.406(13)
N3	C15	1.353(12)
N3	C16	1.415(12)
N4	C15	1.313(12)
N4	C18	1.371(13)
N5	N6	1.239(11)
N5	C18	1.384(13)
N6	C19	1.425(13)
C1	C2	1.459(14)
C1	C6	1.430(13)
C2	C3	1.371(15)
C2	C7	1.61(4)
C2	C7A	1.46(5)
C3	C4	1.396(15)
C4	C5	1.361(14)
C4	C11	1.551(15)
C5	C6	1.453(14)
C7	C8	1.510(19)
C7	C9	1.500(19)
C7	C10	1.503(19)
C11	C12	1.551(18)
C11	C13	1.521(15)
C11	C14	1.541(18)
C16	C17	1.337(13)
C17	C18	1.430(14)
C19	C20	1.411(14)
C19	C24	1.427(13)
C20	C21	1.376(14)
C21	C22	1.406(15)
C21	C25	1.542(14)
C21	C25A	1.543(16)
C22	C23	1.367(16)
C23	C24	1.459(14)
C23	C29	1.528(15)
C25	C27	1.530(14)
C25	C28	1.526(13)
C25	C26	1.532(14)
C26A	C25A	1.531(15)
C29	C30	1.581(15)
C29	C31	1.502(16)
C29	C32	1.522(15)

Atom	Atom	Length/Å
Co2	O3[2]	1.887(6)
Co2	O4	1.886(6)
Co2	N7[2]	1.866(7)
Co2	N9[2]	1.917(8)
Co2	N10	1.956(8)
Co2	N12	1.861(7)
O3	C33	1.288(10)
O4	C56	1.356(10)
N7	N8	1.296(10)
N7	C38	1.350(11)
N8	C48	1.387(12)
N9	C47	1.371(11)
N9	C48	1.432(11)
N10	C47	1.332(11)
N10	C50	1.390(11)
N11	N12	1.270(10)
N11	C50	1.392(12)
N12	C51	1.394(12)
C33	C34	1.437(13)
C33	C38	1.421(12)
C34	C35	1.378(14)
C34	C39	1.541(14)
C35	C36	1.423(15)
C36	C37	1.387(13)
C36	C43	1.531(15)
C37	C38	1.381(12)
C39	C40	1.543(16)
C39	C41	1.500(16)
C39	C42	1.543(16)
C43	C44	1.494(18)
C43	C45	1.537(18)
C43	C46	1.576(16)
C48	C49	1.341(12)
C49	C50	1.353(12)
C51	C52	1.401(12)
C51	C56	1.361(12)
C52	C53	1.359(13)
C53	C54	1.423(13)
C53	C57	1.542(12)
C54	C55	1.355(13)
C55	C56	1.437(13)
C55	C61	1.545(14)
C57	C58	1.528(15)
C57	C59	1.548(14)
C57	C60	1.521(15)
C61	C62	1.535(14)
C61	C63	1.541(15)
C61	C64	1.511(15)
C25A	C28A	1.531(15)
C25A	C27A	1.534(15)
C7A	C10A	1.58(3)

Atom	Atom	Length/Å
C7A	C8A	1.58(3)
C7A	C9A	1.57(3)

----
[1]1/2+y,1/2-x,3/2-z; [2]+y,1-x,1-z

Atom	Atom	Atom	Angle/°
O1[1]	Co1	N3[1]	165.1(3)
O1[1]	Co1	N4	89.4(3)
O2	Co1	O1[1]	90.7(3)
O2	Co1	N3[1]	89.7(3)
O2	Co1	N4	164.6(3)
N1[1]	Co1	O1[1]	84.0(3)
N1[1]	Co1	O2	90.1(3)
N1[1]	Co1	N3[1]	81.1(4)
N1[1]	Co1	N4	105.2(4)
N1[1]	Co1	N6	173.8(4)
N3[1]	Co1	N4	94.2(3)
N6	Co1	O1[1]	91.4(3)
N6	Co1	O2	85.7(3)
N6	Co1	N3[1]	103.4(4)
N6	Co1	N4	78.9(4)
C1	O1	Co1[2]	111.6(6)
C24	O2	Co1	113.3(6)
N2	N1	Co1[2]	122.9(7)
N2	N1	C6	121.3(8)
C6	N1	Co1[2]	115.2(7)
N1	N2	C16	108.3(8)
C15	N3	Co1[2]	136.1(7)
C15	N3	C16	114.0(9)
C16	N3	Co1[2]	109.9(7)
C15	N4	Co1	134.7(8)
C15	N4	C18	116.8(9)
C18	N4	Co1	108.5(7)
N6	N5	C18	107.1(9)
N5	N6	Co1	125.2(7)
N5	N6	C19	122.9(8)
C19	N6	Co1	111.3(6)
O1	C1	C2	125.0(9)
O1	C1	C6	116.5(9)
C6	C1	C2	118.5(9)
C1	C2	C7	120.0(11)
C3	C2	C1	115.2(9)
C3	C2	C7	124.6(11)
C3	C2	C7A	128.0(14)
C7A	C2	C1	115.2(13)
C2	C3	C4	127.0(10)
C3	C4	C11	118.9(9)
C5	C4	C3	119.2(10)
C5	C4	C11	121.8(10)
C4	C5	C6	118.2(10)
N1	C6	C1	112.4(8)
N1	C6	C5	126.1(9)
C1	C6	C5	121.5(9)
C8	C7	C2	101.5(17)
C9	C7	C2	108(2)
C9	C7	C8	111.6(14)
C9	C7	C10	111.8(14)
C10	C7	C2	112(2)
C10	C7	C8	111.8(15)

Atom	Atom	Atom	Angle/°
C4	C11	C12	107.2(10)
C13	C11	C4	111.4(10)
C13	C11	C12	108.8(10)
C13	C11	C14	105.8(12)
C14	C11	C4	111.0(9)
C14	C11	C12	112.7(11)
N4	C15	N3	127.6(10)
N2	C16	N3	117.6(9)
C17	C16	N2	118.8(9)
C17	C16	N3	123.6(10)
C16	C17	C18	116.5(10)
N4	C18	N5	119.8(9)
N4	C18	C17	121.4(10)
N5	C18	C17	118.7(9)
N6	C19	C24	112.1(8)
C20	C19	N6	122.4(9)
C20	C19	C24	125.5(10)
C21	C20	C19	117.1(10)
C20	C21	C22	118.9(9)
C20	C21	C25	122.0(10)
C20	C21	C25A	114.2(15)
C22	C21	C25	118.7(10)
C22	C21	C25A	124.7(15)
C23	C22	C21	125.7(9)
C22	C23	C24	117.5(9)
C22	C23	C29	126.2(9)
C24	C23	C29	116.2(9)
O2	C24	C19	117.2(9)
O2	C24	C23	127.6(9)
C19	C24	C23	115.2(9)
C27	C25	C21	105.2(13)
C27	C25	C26	109.5(9)
C28	C25	C21	113.0(13)
C28	C25	C27	109.9(9)
C28	C25	C26	110.1(9)
C26	C25	C21	109.0(16)
C23	C29	C30	111.0(9)
C31	C29	C23	110.4(9)
C31	C29	C30	108.3(9)
C31	C29	C32	114.0(11)
C32	C29	C23	108.6(9)
C32	C29	C30	104.3(10)
O3[3]	Co2	N9[3]	164.4(3)
O3[3]	Co2	N10	89.6(3)
O4	Co2	O3[3]	90.1(3)
O4	Co2	N9[3]	89.9(3)
O4	Co2	N10	165.6(3)
N7[3]	Co2	O3[3]	83.8(3)
N7[3]	Co2	O4	88.8(3)
N7[3]	Co2	N9[3]	80.6(3)
N7[3]	Co2	N10	105.5(3)
N9[3]	Co2	N10	94.3(3)
N12	Co2	O3[3]	92.0(3)

Atom	Atom	Atom	Angle/°
N12	Co2	O4	85.9(3)
N12	Co2	N7[3]	173.3(3)
N12	Co2	N9[3]	103.5(3)
N12	Co2	N10	79.7(3)
C33	O3	Co2[4]	112.8(6)
C56	O4	Co2	109.5(5)
N8	N7	Co2[4]	122.4(6)
N8	N7	C38	122.4(7)
C38	N7	Co2[4]	114.6(6)
N7	N8	C48	109.5(8)
C47	N9	Co2[4]	135.5(6)
C47	N9	C48	113.2(8)
C48	N9	Co2[4]	111.3(6)
C47	N10	Co2	132.7(6)
C47	N10	C50	117.0(8)
C50	N10	Co2	110.2(6)
N12	N11	C50	109.1(7)
N11	N12	Co2	123.3(6)
N11	N12	C51	123.0(7)
C51	N12	Co2	112.4(6)
O3	C33	C34	124.5(8)
O3	C33	C38	117.6(8)
C38	C33	C34	118.0(8)
C33	C34	C39	119.8(8)
C35	C34	C33	116.7(8)
C35	C34	C39	123.4(9)
C34	C35	C36	125.1(9)
C35	C36	C43	118.8(9)
C37	C36	C35	117.5(9)
C37	C36	C43	123.6(9)
C38	C37	C36	119.3(9)
N7	C38	C33	111.1(7)
N7	C38	C37	125.4(8)
C37	C38	C33	123.4(8)
C34	C39	C40	109.0(9)
C34	C39	C42	110.0(9)
C41	C39	C34	108.6(9)
C41	C39	C40	109.7(9)
C41	C39	C42	108.5(11)
C42	C39	C40	111.0(11)
C36	C43	C45	106.9(10)
C36	C43	C46	109.8(9)
C44	C43	C36	111.8(11)
C44	C43	C45	109.9(12)
C44	C43	C46	110.1(11)
C45	C43	C46	108.3(12)
N10	C47	N9	126.2(9)
N8	C48	N9	115.8(8)

Atom	Atom	Atom	Angle/°
C49	C48	N8	121.3(8)
C49	C48	N9	122.8(9)
C48	C49	C50	119.1(9)
N10	C50	N11	117.3(8)
C49	C50	N10	121.6(9)
C49	C50	N11	121.1(8)
N12	C51	C52	123.1(8)
C56	C51	N12	112.5(8)
C56	C51	C52	124.3(9)
C53	C52	C51	117.2(9)
C52	C53	C54	118.7(9)
C52	C53	C57	121.7(9)
C54	C53	C57	119.5(8)
C55	C54	C53	125.1(9)
C54	C55	C56	115.3(9)
C54	C55	C61	123.9(9)
C56	C55	C61	120.9(8)
O4	C56	C51	118.9(8)
O4	C56	C55	121.7(8)
C51	C56	C55	119.3(8)
C53	C57	C59	109.5(8)
C58	C57	C53	112.7(9)
C58	C57	C59	107.7(9)
C60	C57	C53	110.8(9)
C60	C57	C58	110.8(10)
C60	C57	C59	105.0(9)
C62	C61	C55	112.3(8)
C62	C61	C63	109.3(9)
C63	C61	C55	109.7(9)
C64	C61	C55	108.8(9)
C64	C61	C62	105.6(8)
C64	C61	C63	111.2(9)
C26A	C25A	C21	106(4)
C26A	C25A	C28A	109.6(12)
C26A	C25A	C27A	109.3(12)
C28A	C25A	C21	112(3)
C28A	C25A	C27A	109.4(12)
C27A	C25A	C21	111(3)
C2	C7A	C10A	109(2)
C2	C7A	C8A	113(2)
C2	C7A	C9A	114(3)
C10A	C7A	C8A	106.6(19)
C9A	C7A	C10A	106.9(19)
C9A	C7A	C8A	107.1(19)

––––

[1]1/2+y,1/2-x,3/2-z; [2]1/2-y,-1/2+x,3/2-z; [3]+y,1-x,1-z; [4]1-y,+x,1-z

One t-butyl group was disordered and was modelled in two orientations using mild restraints on bond lengths to maintain reasonable geometries. The ratio of the occupancies of the two disordered fragments is approximately 0.63:0.37.

Figure S10. Molecular structure of the second crystallographically independent molecule of **1** (displacement ellipsoids at 30% probability) in the asymmetric unit. H atoms and solvent omitted for clarity.

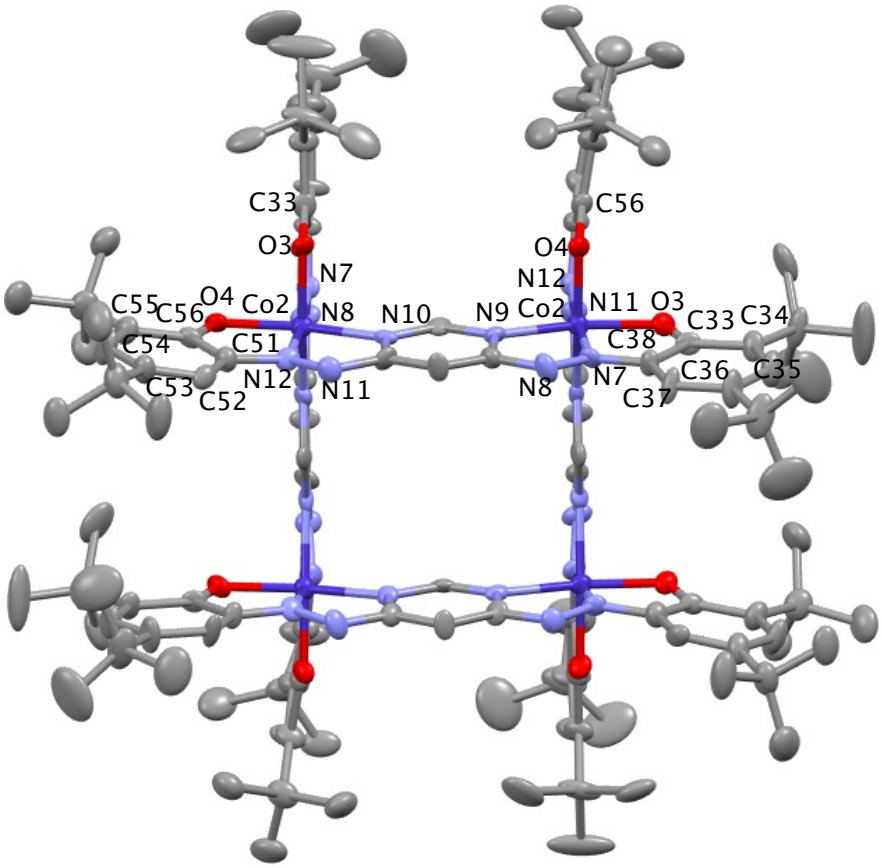

Figure S11. Thermogravimetric analysis of **1**.

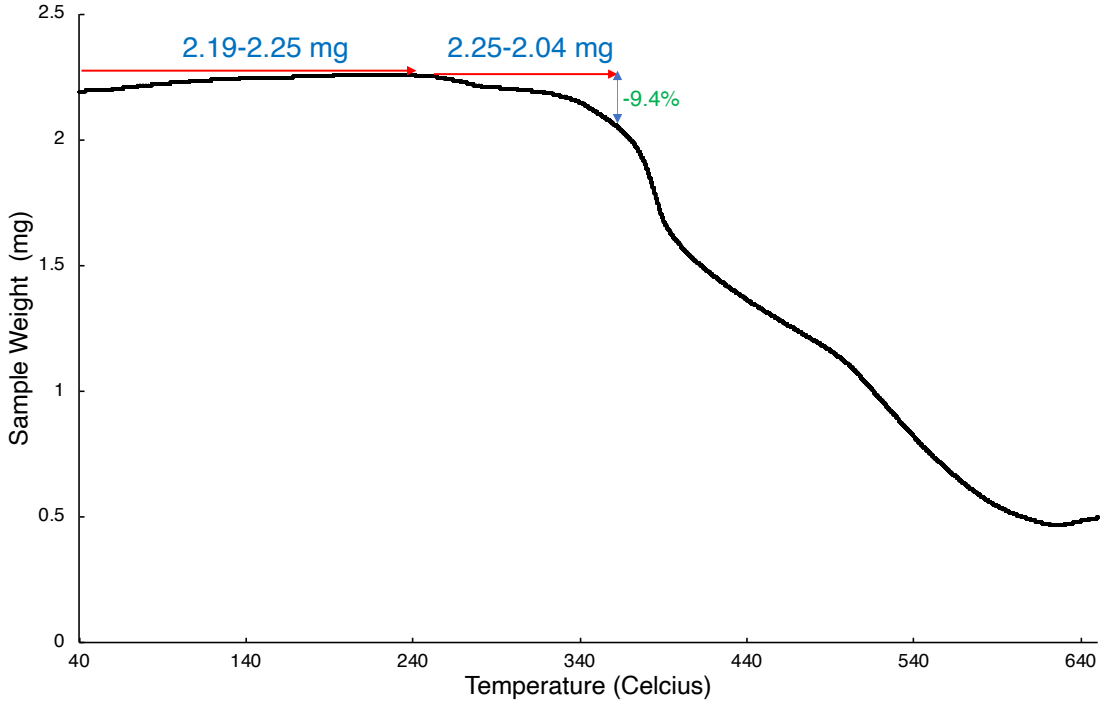

Figure S12. UV-vis-NIR spectra of **1** (CH_2Cl_2) obtained over a 24 h period.

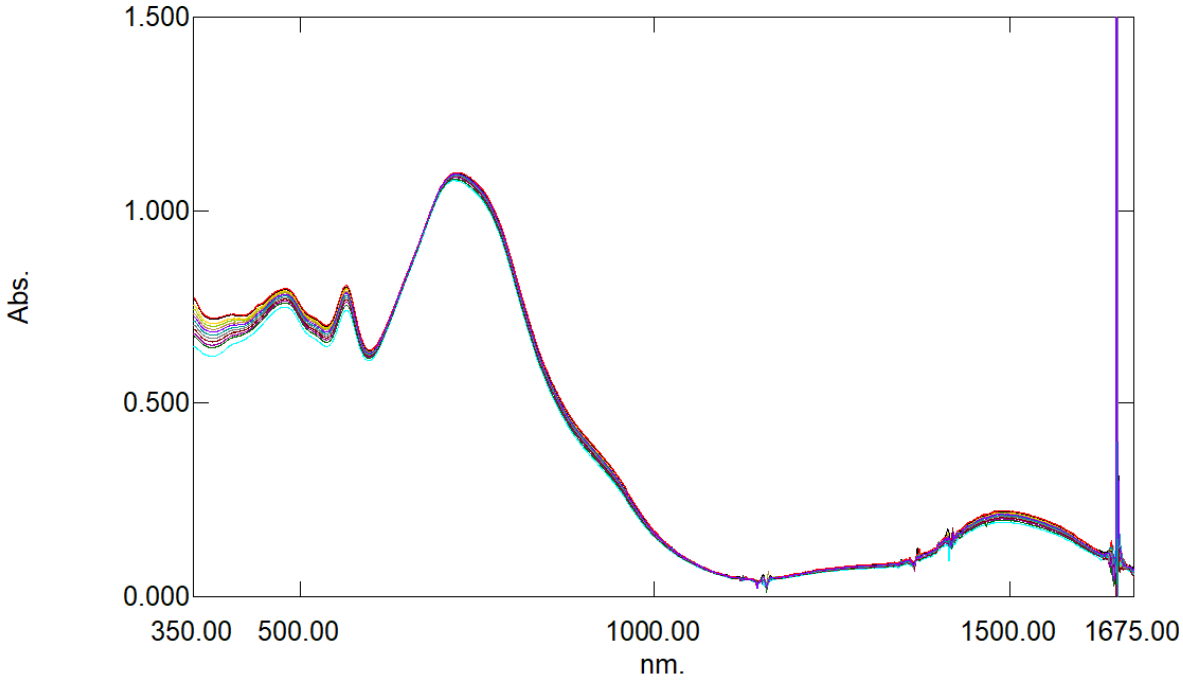

Figure S13. (Top) Positive ion mode ESI mass spectrum of **1** (fresh solution). (Bottom) Experimental and calculated isotopic distribution of the M^+ cluster of peaks from the ESI.

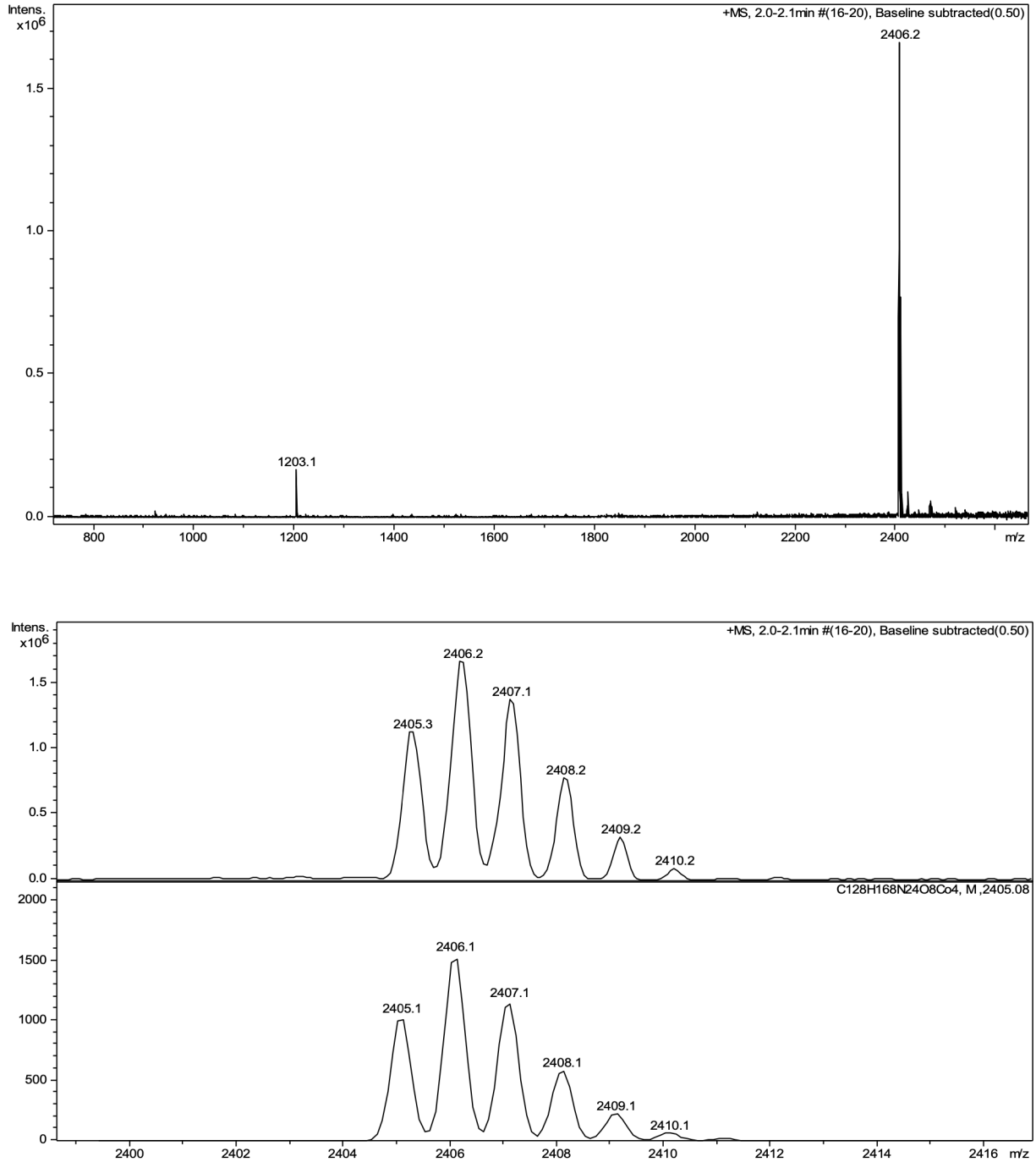

Figure S14. Positive ion mode ESI mass spectrum of **1** (in solution for 24 hours).

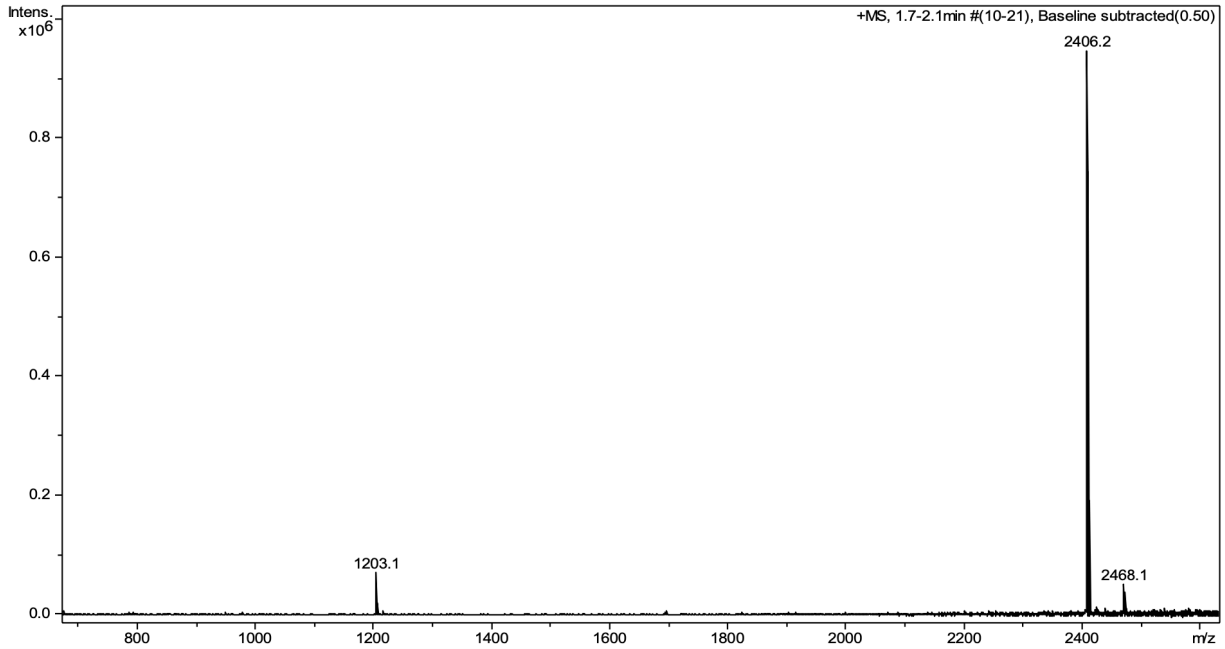

Figure S15. (Top) Variable temperature UV-visible-NIR spectra of **1** in THF (298 – 333 K). (Bottom) Variable temperature UV-visible-NIR spectra of **1** in Toluene (298 – 373 K).

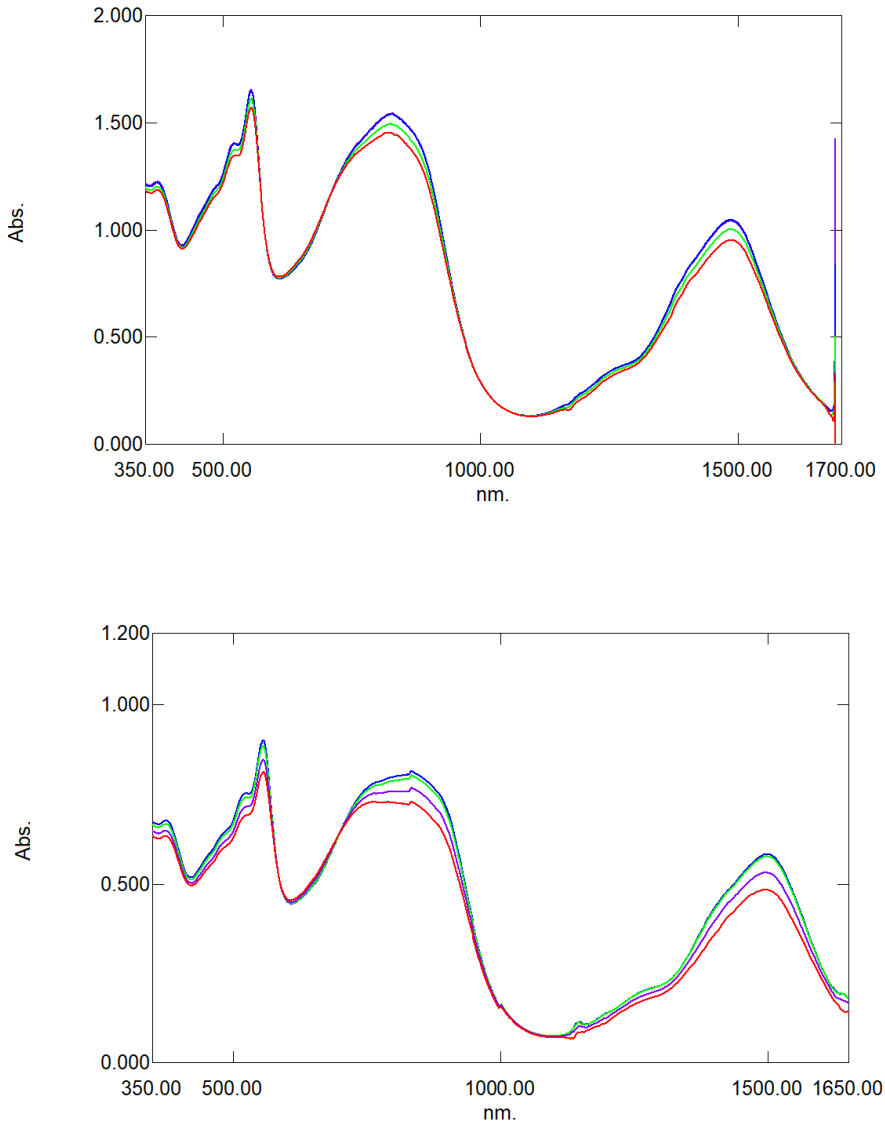

Figure S16. Cyclic voltammogram of **1** in CH_2Cl_2 (containing 0.5 M Bu_4NPF_6). Scan rate 100 mV/s. Potential window = +1000 mV to -2000 mV.

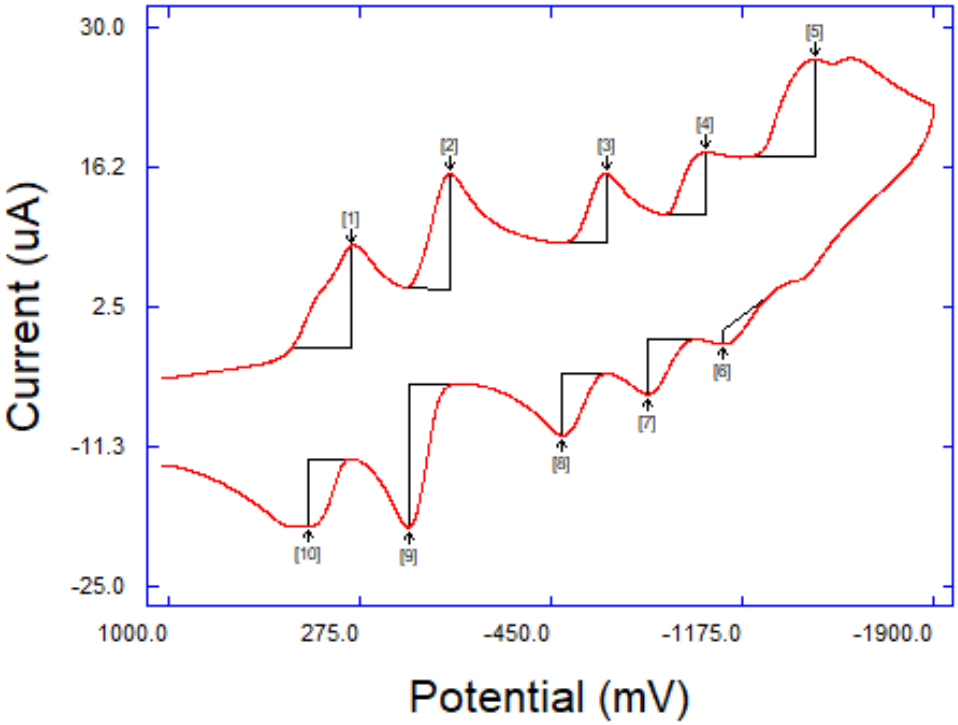

Table S5. Electrochemical data for complex **1**.

E_{pa} & E_{pc} from Figure S16	$E_{1/2}$ (V) vs Ag/AgCl
1 & 10	+0.39 V (qr)
2 & 9	+0.01 V (qr)
3 & 8	-0.58 V (qr)
4 & 7	-0.93 V (irr)
5 & 6	-1.3 V (irr)

***qr = quasi-reversible; irr = irreversible**

Table S6. Crystallographic parameters for **2** (CCDC 1922364).

Formula	$C_{40}H_{54}ClCoN_6O_7$
$D_{calc.}$/ g cm^{-3}	1.180
μ/mm^{-1}	0.476
Formula Weight	824.40
Colour	black
Shape	rod
Size/mm^3	0.26×0.13×0.10
T/K	100(2)
Crystal System	monoclinic
Space Group	$C2/c$
a/Å	25.049(2)
b/Å	10.4508(9)
c/Å	36.994(3)
α/°	90
β/°	106.546(5)
γ/°	90
V/Å^3	9283.3(15)
Z	8
Z'	1
Wavelength/Å	0.71073
Radiation type	MoK$_\alpha$
Θ_{min}/°	2.125
Θ_{max}/°	26.413
Measured Refl.	9241
Independent Refl.	9241
Reflections with I > 2(I)	8391
R_{int}	0.082
Parameters	602
Restraints	689
Largest Peak	0.978
Deepest Hole	-0.461
GooF	1.112
wR_2 (all data)	0.1812
wR_2	0.1786
R_1 (all data)	0.0835
R_1	0.0772

Table S7. Bond distances (Å) and angles (°) for **2**.

Atom	Atom	Length/Å
Co1	O1	1.904(3)
Co1	O2	1.902(3)
Co1	N1	1.859(4)
Co1	N3	1.919(4)
Co1	N4	1.862(4)
Co1	N6	1.919(4)
O1	C1	1.319(5)
O2	C21	1.327(5)
N1	N2	1.290(5)
N1	C6	1.376(6)
N2	C15	1.407(6)
N3	C15	1.370(6)
N3	C19	1.332(6)
N4	N5	1.284(5)
N4	C20	1.373(6)
N5	C34	1.398(6)
N6	C34	1.384(6)
N6	C38	1.332(6)
C1	C2	1.432(6)
C1	C6	1.425(6)
C2	C3	1.388(6)
C2	C7	1.534(6)
C3	C4	1.439(7)
C4	C5	1.362(7)
C4	C11	1.549(6)
C5	C6	1.425(6)
C7	C8	1.538(7)
C7	C9	1.547(7)
C7	C10	1.538(7)
C11	C12	1.531(7)
C11	C13	1.537(7)
C11	C14	1.534(7)
C15	C16	1.393(7)
C16	C17	1.395(7)
C17	C18	1.391(8)

Atom	Atom	Length/Å
C18	C19	1.397(7)
C20	C21	1.424(7)
C20	C25	1.423(6)
C21	C22	1.429(6)
C22	C23	1.386(6)
C22	C26	1.535(6)
C23	C24	1.428(7)
C24	C25	1.367(7)
C24	C30	1.550(6)
C26	C27	1.549(7)
C26	C28	1.538(7)
C26	C29	1.530(7)
C30	C31	1.538(9)
C30	C32	1.520(8)
C30	C33	1.529(7)
C34	C35	1.381(7)
C35	C36	1.392(8)
C36	C37	1.389(8)
C37	C38	1.395(7)
Cl1	O3	1.4423
Cl1	O4	1.4436
Cl1	O5	1.4411
Cl1	O6	1.4435
Cl1A	O3A	1.443(14)
Cl1A	O4A	1.447(14)
Cl1A	O5A	1.439(15)
Cl1A	O6A	1.445(14)
Cl1B	O3B	1.418(14)
Cl1B	O4B	1.420(14)
Cl1B	O5B	1.426(15)
Cl1B	O6B	1.422(14)
O7	C40	1.432(16)
C39	C40	1.500(15)
C39	C40A	1.498(11)
C40A	O7A	1.431(12)

Atom	Atom	Atom	Angle/°
O1	Co1	N3	166.77(16)
O1	Co1	N6	88.63(15)
O2	Co1	O1	91.66(13)
O2	Co1	N3	88.60(15)
O2	Co1	N6	166.91(16)
N1	Co1	O1	85.58(16)
N1	Co1	O2	94.52(16)
N1	Co1	N3	81.22(17)
N1	Co1	N4	178.88(19)
N1	Co1	N6	98.55(17)
N4	Co1	O1	93.37(15)
N4	Co1	O2	85.88(15)
N4	Co1	N3	99.84(17)

Atom	Atom	Atom	Angle/°
N4	Co1	N6	81.03(17)
N6	Co1	N3	94.09(16)
C1	O1	Co1	110.4(3)
C21	O2	Co1	110.1(3)
N2	N1	Co1	121.5(3)
N2	N1	C6	124.3(4)
C6	N1	Co1	114.2(3)
N1	N2	C15	108.7(4)
C15	N3	Co1	110.8(3)
C19	N3	Co1	130.4(3)
C19	N3	C15	118.7(4)
N5	N4	Co1	121.5(3)
N5	N4	C20	124.5(4)

Atom	Atom	Atom	Angle/°
C20	N4	Co1	114.0(3)
N4	N5	C34	109.4(4)
C34	N6	Co1	110.8(3)
C38	N6	Co1	129.8(3)
C38	N6	C34	119.3(4)
O1	C1	C2	123.1(4)
O1	C1	C6	119.0(4)
C6	C1	C2	117.9(4)
C1	C2	C7	120.0(4)
C3	C2	C1	116.4(4)
C3	C2	C7	123.5(4)
C2	C3	C4	125.4(4)
C3	C4	C11	121.2(4)
C5	C4	C3	118.1(4)
C5	C4	C11	120.7(4)
C4	C5	C6	118.4(4)
N1	C6	C1	110.8(4)
N1	C6	C5	125.5(4)
C5	C6	C1	123.7(4)
C2	C7	C8	110.5(4)
C2	C7	C9	109.7(4)
C2	C7	C10	111.2(4)
C8	C7	C9	109.6(4)
C10	C7	C8	107.7(4)
C10	C7	C9	108.1(4)
C12	C11	C4	112.6(4)
C12	C11	C13	109.1(5)
C12	C11	C14	108.4(5)
C13	C11	C4	109.2(4)
C14	C11	C4	108.8(4)
C14	C11	C13	108.7(4)
N3	C15	N2	117.8(4)
N3	C15	C16	122.1(5)
C16	C15	N2	120.1(4)
C15	C16	C17	118.2(5)
C18	C17	C16	119.7(5)
C17	C18	C19	118.6(5)
N3	C19	C18	122.6(4)
N4	C20	C21	111.0(4)
N4	C20	C25	125.4(4)
C25	C20	C21	123.5(4)
O2	C21	C20	119.0(4)
O2	C21	C22	122.3(4)
C20	C21	C22	118.6(4)
C21	C22	C26	121.0(4)
C23	C22	C21	115.3(4)

Atom	Atom	Atom	Angle/°
C23	C22	C26	123.7(4)
C22	C23	C24	126.5(5)
C23	C24	C30	118.9(4)
C25	C24	C23	118.0(4)
C25	C24	C30	123.0(4)
C24	C25	C20	117.9(4)
C22	C26	C27	108.9(4)
C22	C26	C28	109.9(4)
C28	C26	C27	110.6(4)
C29	C26	C22	111.7(4)
C29	C26	C27	107.4(4)
C29	C26	C28	108.4(4)
C31	C30	C24	108.2(4)
C32	C30	C24	109.7(4)
C32	C30	C31	109.5(5)
C32	C30	C33	109.4(5)
C33	C30	C24	111.0(4)
C33	C30	C31	108.9(5)
N6	C34	N5	117.1(4)
C35	C34	N5	121.3(4)
C35	C34	N6	121.5(5)
C34	C35	C36	118.2(5)
C37	C36	C35	120.5(5)
C36	C37	C38	118.4(5)
N6	C38	C37	122.0(5)
O3	Cl1	O4	109.5
O3	Cl1	O6	109.5
O5	Cl1	O3	109.5
O5	Cl1	O4	109.4
O5	Cl1	O6	109.6
O6	Cl1	O4	109.3
O3A	Cl1A	O4A	109.6(6)
O3A	Cl1A	O6A	109.2(6)
O5A	Cl1A	O3A	109.7(6)
O5A	Cl1A	O4A	109.6(6)
O5A	Cl1A	O6A	109.6(6)
O6A	Cl1A	O4A	109.0(6)
O3B	Cl1B	O4B	109.8(6)
O3B	Cl1B	O5B	109.4(6)
O3B	Cl1B	O6B	109.6(6)
O4B	Cl1B	O5B	109.4(6)
O4B	Cl1B	O6B	109.5(6)
O6B	Cl1B	O5B	109.0(6)
O7	C40	C39	134(7)
O7A	C40A	C39	113.1(9)

Figure S17. Molecular structure of **2** (displacement ellipsoids at 30% probability). H atoms and solvent omitted for clarity.

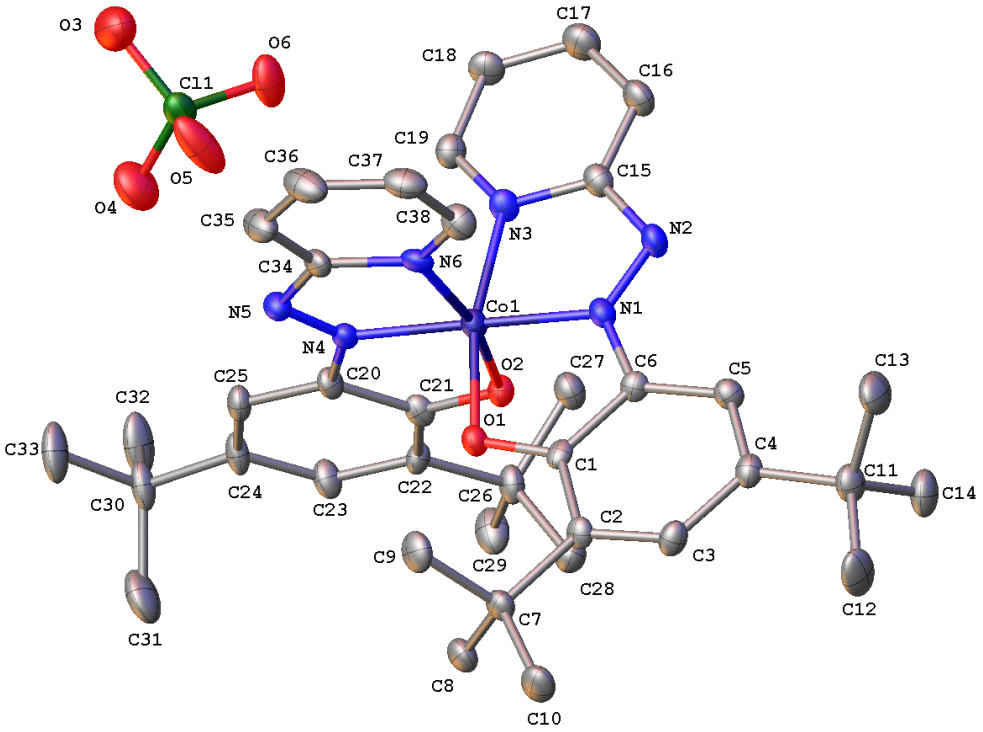

Figure S18. ^{1}H NMR spectrum of **2** ($CDCl_3$).

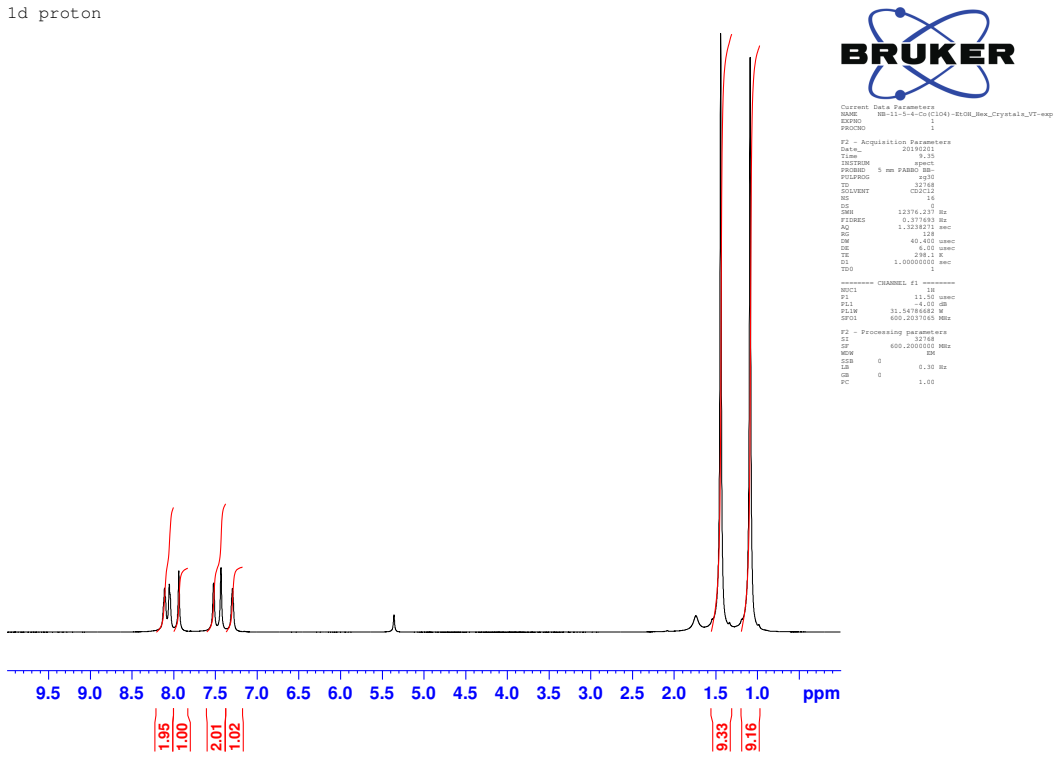

Figure S19. ^{13}C NMR spectrum of **2** ($CDCl_3$).

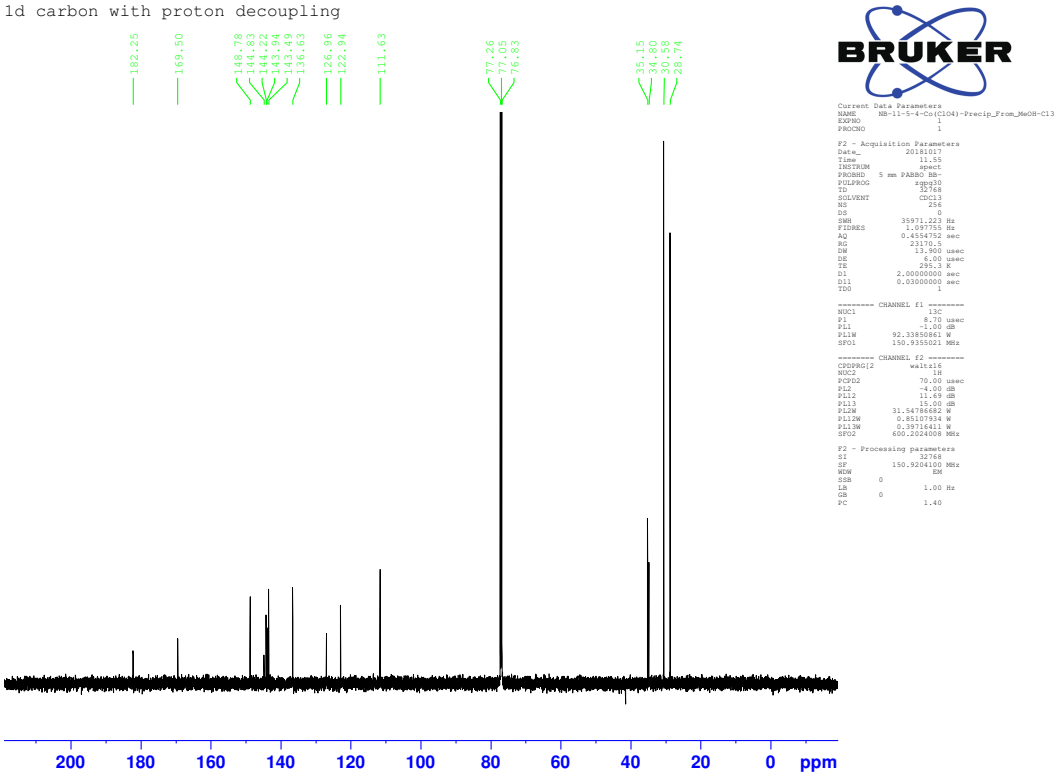

Figure S20. ESI mass spectrum (positive ion mode) of **2**.

MS Instrument: Bruker HCTplus Ion-Trap

Sample Name: NB-11-4-4 **Ion Source Type(Polarity)**: ESI+/-

File Name: MLH2111 **Solvent** : DCM/MeOH

Please read through the 4-page report.

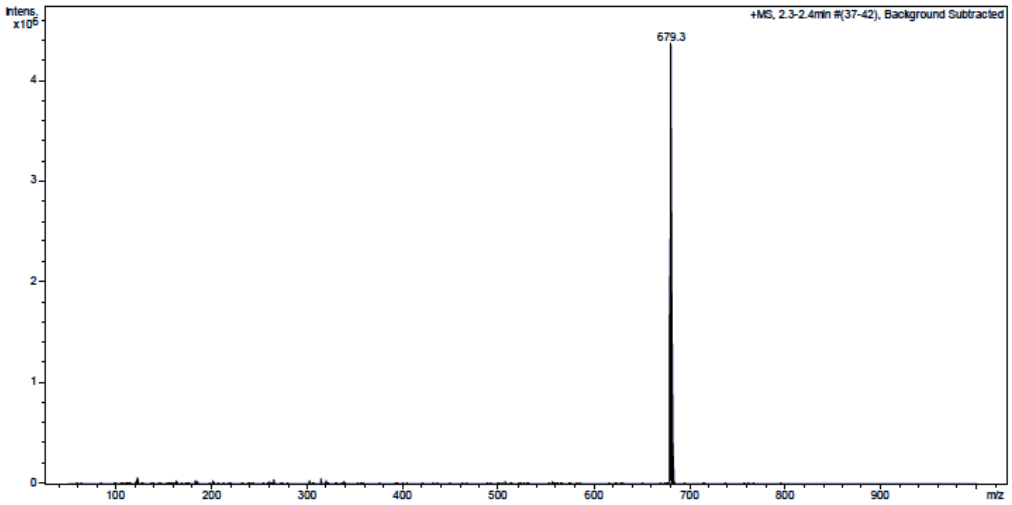

MS Instrument: Bruker HCTplus Ion-Trap

Sample Name: NB-11-4-4 **Ion Source Type(Polarity)**: ESI+/-

File Name: MLH2111 **Solvent** : DCM/MeOH

Please read through the 4-page report.

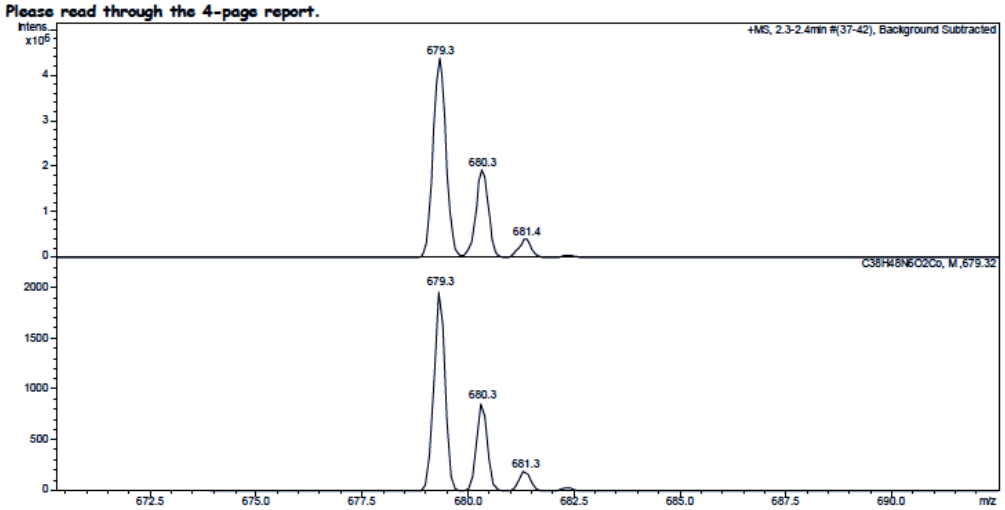

Table S8. Energies (E) and spin expectation values ($<S^2>$) for the $S = 2$ and broken symmetry $M_S = 0$ states (ααββ and αβαβ configurations) of complex **1** (BP86/def2-SVP).

State	E (hartrees)	ΔE (cm^{-1})	$<S^2>$
$S = 2$	–12419.194375	59.4	6.0157
$M_S = 0$ (BS, ααββ)	–12419.194646	0	1.9181
$M_S = 0$ (BS, αβαβ)	–12419.194257	85.4	1.9671

Exchange interactions, $J_{\text{neighboring}}$ and $J_{\text{face-to-face}}$, of complex **1** was analytically considered by the following spin-Hamiltonian ($S_A = S_B = S_C = S_D = 1/2$):

$$H = -2J_{\text{neighboring}} (S_A S_B + S_B S_C + S_C S_D + S_D S_A) - 2J_{\text{face-to-face}} (S_A S_C + S_B S_D)$$

The exchange interactions are given by

$J_{\text{neighboring}} = [E(\text{BS, αβαβ}) - E(S{=}2)]/4$

and $J_{\text{face-to-face}} = [E(\text{BS, ααββ}) - E(\text{BS, αβαβ}) + 2J_{\text{neighboring}}]/2$.

Figure S21. Spin density (red = alpha spin density and blue = beta spin density) in the $S = 2$ state of 1 (BP86/def2-SVP).

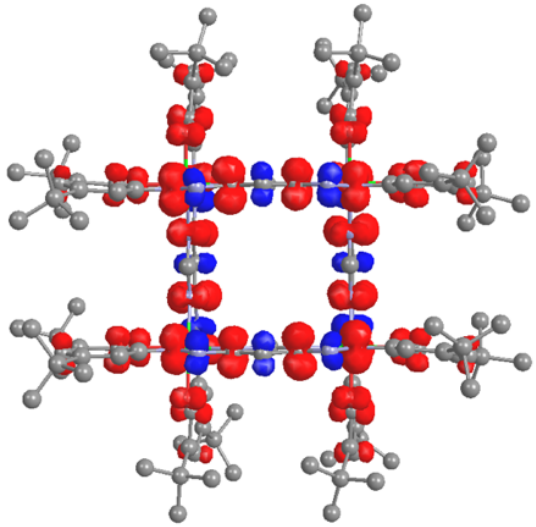

Figure S22. Temperature dependence of X-band EPR spectra of complex **1.** (a) Normalized spectra between 4 K and 290 K, (b) Spectra between 100 K and 300 K.

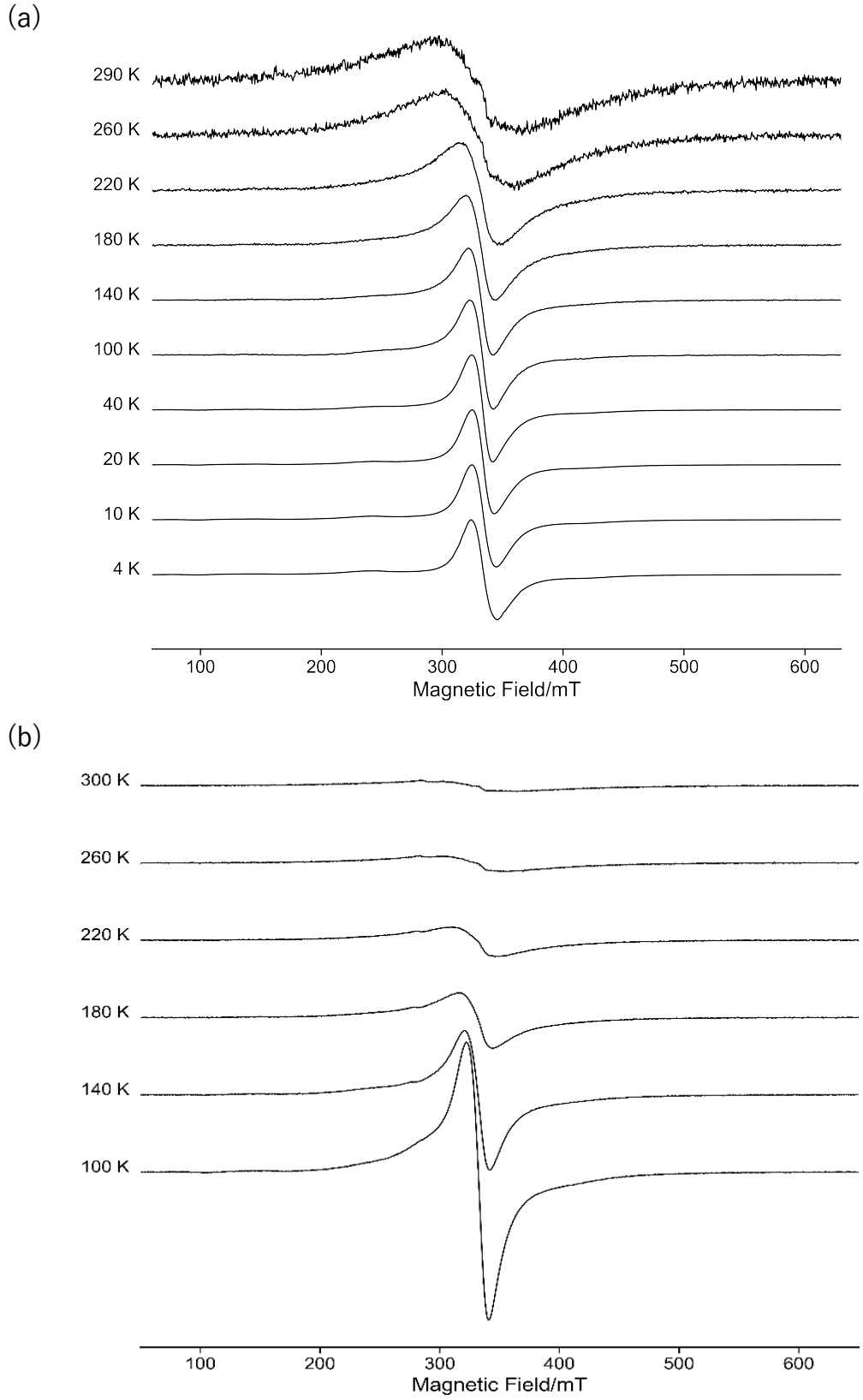

Figure S23. Variable temperature infrared spectra of **1** (KBr pellet).

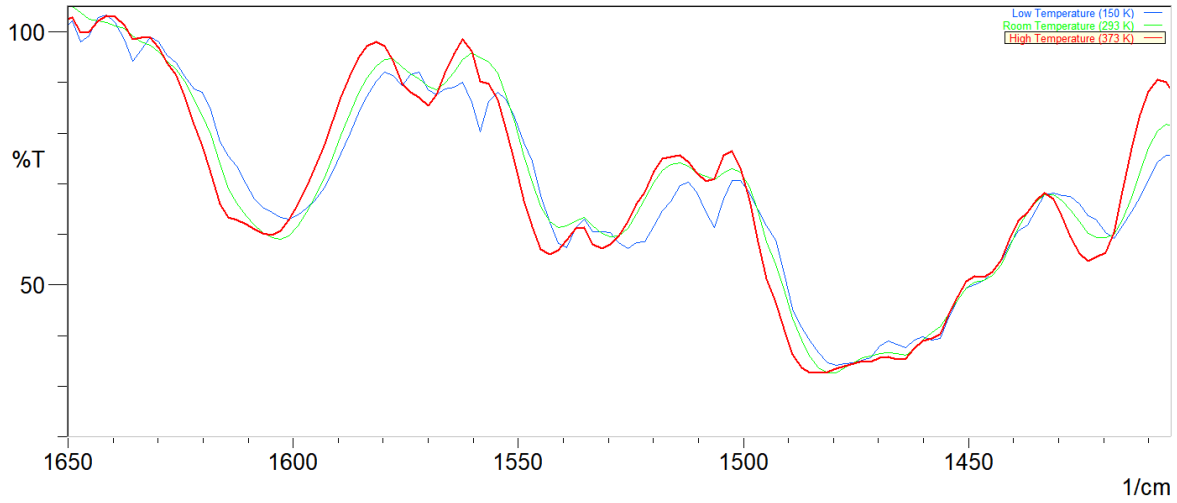

Figure S24. Variable temperature infrared spectra of **1** (KBr pellet).

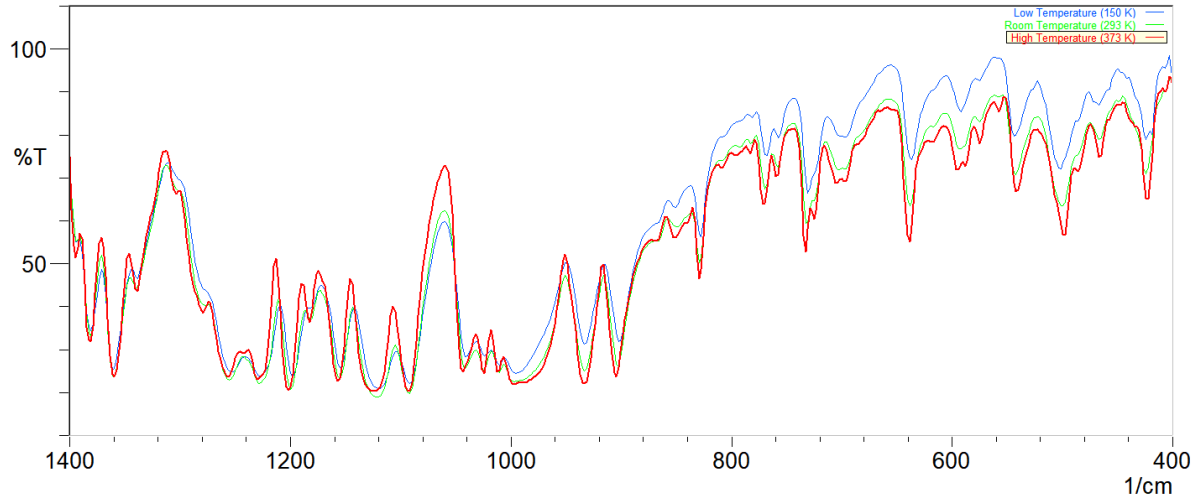

References in the Supporting Information

(1) Neese, F. The ORCA Program System. *Wiley Interdiscip. Rev. Comput. Mol. Sci.* **2012**, *2*, 73–78.
(2) Becke, A. D. *J. Chem. Phys.* **1993**, *98*, 5648.
(3) Vosko, S. H.; Wilk, L.; Nusair, M. *Can. J. Phys.* **1980**, *58*, 1200–1211.
(4) Perdew, J. P. *Phys. Rev. B* **1986**, *33*, 8822–8824.
(5) Schäfer, A.; Horn, H.; Ahlrichs, R. *J. Chem. Phys.* **1992**, *97*, 2571–2577.
(6) Weigend, F.; Ahlrichs, R. *Phys. Chem. Chem. Phys.* **2005**, *7*, 3297–3305.
(7) Ginsberg, A. P. *J. Am. Chem. Soc.* **1980**, *102*, 111–117.
(8) Noodleman, L. *J. Chem. Phys.* **1981**, *74*, 5737–5743.
(9) Noodleman, L.; Davidson, E. R. *Chem. Phys*. **1986**, *109*, 131–143.
(10) Tenderholt, A. L. QMForge, Version 2.4, Http://Qmforge.Sourceforge.Net.